

**Soil nutrient competitive traits of plants, microbes, and mineral surfaces explain
nutrient acquisition in tropical experimental manipulations**

Qing Zhu^{1*}, William J. Riley¹, Jinyun Tang¹, Charles D. Koven¹

¹ Climate Sciences Department, Earth Sciences Division, Lawrence Berkeley National
Laboratory, Berkeley, CA 94720

* Correspondence to: Q. Zhu (qzhu@lbl.gov)

Abstract

Soil is a complex system where biotic (*e.g.*, plant roots, micro-organisms) and
abiotic (*e.g.*, mineral surfaces) consumers compete for resources necessary for life (*e.g.*,
nitrogen, phosphorus). This competition is ecologically significant, since it regulates the
dynamics of soil nutrients and controls aboveground plant productivity. Here we develop,
calibrate, and test a nutrient competition model that accounts for multiple soil nutrients
interacting with multiple biotic and abiotic consumers. As applied here for tropical
forests, the Nutrient COMpetition model (N-COM) includes three primary soil nutrients
(NH_4^+ , NO_3^- , and PO_x (representing the sum of PO_4^{3-} , HPO_4^{2-} , and H_2PO_4^-)) and five
potential competitors (plant roots, decomposing microbes, nitrifiers, denitrifiers, and
mineral surfaces). The competition is formulated with a quasi-steady-state chemical
equilibrium approximation to account for substrate (multiple substrates share one
consumer) and consumer (multiple consumers compete for one substrate) effects. N-
COM successfully reproduced observed soil heterotrophic respiration, N_2O emissions,
free phosphorus, sorbed phosphorus, and NH_4^+ pools at a tropical forest site (Tapajos).
The overall model posterior uncertainty was moderately well constrained. Our sensitivity
analysis revealed that soil nutrient competition was primarily regulated by consumer-

24 substrate affinity rather than environmental factors such as soil temperature or soil
25 moisture. Our results imply that under strong nutrient limitation, relative competitiveness
26 depends strongly on the competitor functional traits (affinity and nutrient carrier enzyme
27 abundance). We then applied the N-COM model to analyze field nitrogen and
28 phosphorus perturbation experiments in two tropical forest sites (in Hawaii and Puerto
29 Rico) not used in model development or calibration. Under soil inorganic nitrogen and
30 phosphorus elevated conditions, the model accurately replicated the experimentally
31 observed competition among different nutrient consumers. Although we used as many
32 observations as we could obtain, more nutrient addition experiments in tropical systems
33 would greatly benefit model testing and calibration. In summary, the N-COM model
34 provides an ecologically consistent representation of nutrient competition appropriate for
35 land BGC models integrated in Earth System Models.

1 Introduction

Atmospheric CO₂ concentrations have risen sharply since the pre-industrial era, primarily due to anthropogenic fossil fuel combustion and land use and land cover change [Houghton, 2003; Le Quéré *et al.*, 2013; Marland *et al.*, 2003]. Terrestrial ecosystems mitigate the increasing atmospheric CO₂ trend by absorbing roughly a quarter of anthropogenic CO₂ emissions [Le Quéré *et al.*, 2009]. However, it is still an open question whether the terrestrial CO₂ sink can be sustained [Sokolov *et al.*, 2008; Zaehle *et al.*, 2010], given that plant productivity is generally limited by soil nutrients [Elser *et al.*, 2007; LeBauer and Treseder, 2008; Vitousek and Howarth, 1991] and soil nutrients could be quickly depleted through biogeochemical [Chauhan *et al.*, 1981; Nordin *et al.*, 2001; Shen *et al.*, 2011] and hydrological [Dise and Wright, 1995; Perakis and Hedin, 2002] processes. Therefore, a holistic representation of soil nutrient dynamics is critically important to model the responses of terrestrial ecosystem CO₂ uptake to climate change.

Until recently, land models integrated in Earth System Models (ESMs) have largely ignored the close coupling between soil nutrient dynamics and the carbon cycle, although the impacts of soil nutrients (primarily Nitrogen and Phosphorus) regulating carbon-climate feedback are clearly required in ecosystem biogeochemistry and land models [Zaehle and Dalmonch, 2011; Zhang *et al.*, 2011]. For example, none of the land models in C⁴MIP (Coupled Climate Carbon Cycle Model Intercomparison Project phase 4) had coupled Carbon and Nitrogen dynamics [Friedlingstein *et al.*, 2006]. The current generation of CMIP5 [Anav *et al.*, 2013] models used for the recent IPCC (Intergovernmental Panel on Climate Change) assessment had only two members (CLM4CN: Thornton *et al.* [2007]; and BNU-ESM: [Ji *et al.*, 2014]) that considered

nitrogen regulation of terrestrial carbon dynamics. However, as discussed below, several recent studies have shown that these models had large biases in most of the individual processes important for simulating nutrient dynamics. We therefore believe that, at the global scale, no credible representation of nutrient constraints on terrestrial carbon cycling yet exists in ESMs.

Further, none of the CMIP5 ESMs included a phosphorus cycle, which is likely important for tropical forest carbon budgets [Vitousek and Sanford, 1986]. The recent IPCC report highlights the importance of nitrogen and phosphorus availability on land carbon storage, even though the phosphorus limitation effect is uncertain [Stocker *et al.*, 2013]. Since the next generation of ESMs participating in the CMIP6 synthesis will continue to focus on the impacts of a changing climate on terrestrial CO₂ and abiotic exchanges with the atmosphere [Provides, 2014], developing ecologically realistic and observationally-constrained representations of soil nutrient dynamics and carbon-nutrient interactions in ESMs is critical.

The importance of nutrient limitations in terrestrial ecosystems has been widely demonstrated by nitrogen and phosphorus fertilization experiments [Elser *et al.*, 2007]. For instance, plant Net Primary Production (NPP) is enhanced in plots with nutrient addition [LeBauer and Treseder, 2008]. Similarly, plant growth can be stimulated due to atmospheric nitrogen deposition [Matson *et al.*, 2002]. Boreal forests are strongly limited by nitrogen availability [Vitousek and Howarth, 1991], because low temperatures reduce nitrogen mineralization [Bonan and Cleve, 1992] and N₂ fixation [DeLuca *et al.*, 2008; DeLuca *et al.*, 2002]. In contrast, tropical forests are often phosphorus limited [Vitousek *et al.*, 2010], since tropical soils are old and phosphorus derived from parent material

weathering has been depleted through long-term pedogenesis processes [Vitousek and Farrington, 1997; Walker and Syers, 1976]. In natural ecosystems without external nutrients inputs (e.g., N deposition), soil nitrogen or phosphorus (or both) are likely insufficient to satisfy both plant and microorganism demands [Vitousek and Farrington, 1997]. Plants have to compete with microorganisms and mineral surfaces [Kaye and Hart, 1997; Schimel et al., 1989] to obtain sufficient nutrients to sustain their biological processes (e.g., photosynthesis, respiration). Therefore, it is critical to improve the representation of nutrient competition to accurately model how terrestrial ecosystems will respond to perturbations in soil nutrient dynamics (e.g., from elevated nitrogen deposition or CO₂ fertilization-induced nutrient requirements).

Intense competition between plants and microorganisms is a well-observed phenomenon in nutrient-limited systems [Hodge et al., 2000a; Johnson, 1992; Kaye and Hart, 1997]. Previously, plants were thought to be initial losers in nutrient competition, due to the fact that microbes are more intimately associated with substrates [Woodmansee et al., 1981]. However, increasing observational evidence indicates that plants compete effectively with soil microorganisms [Schimel and Bennett, 2004] under certain circumstances; sometime even outcompeting them and suppressing microbial growth [Hu et al., 2001; J Wang and Lars, 1997]. ¹⁵N isotope studies have also demonstrated that plants can capture a large fraction of added nitrogen [Hodge et al., 2000b; Marion et al., 1982]. In the short term (days to months), plants maintain their competitiveness mainly through (1) establishing mycorrhizal fungi associations [Drake et al., 2011; Rillig et al., 1998], which help plants acquire organic and inorganic forms of nitrogen [Hobbie and Hobbie, 2006; Hodge and Fitter, 2010] and (2) root exudation of extracellular enzymes

that decompose rhizosphere soil organic matter [Phillips *et al.*, 2011]. In the relatively longer term (months to years), morphological adjustment occurs; for example, plants allocate more carbon to fine roots to explore deeper and larger soil volume [Iversen *et al.*, 2011; Jackson *et al.*, 2009]. Finally, over the course of years to decades, plant succession can occur [Medvigy *et al.*, 2009; Moorcroft *et al.*, 2001] and the new plant demography will need to be considered to represent nutrient controls on this time scale.

Given these patterns from the observational literature, nutrient competition is either absent or over-simplified in existing Earth System Models (ESMs). One common representation of plant-microbe competition is that plants compete poorly against microbes in resource acquisition. For example, the O-CN land model [Zaehle and Friend, 2010] assumes that soil decomposing microbes have the priority to immobilize soil mineral nitrogen. After microbes meet their demands, the remaining nitrogen is then available for plant uptake.

Another treatment in ESM land models is that microbial and plant nutrient acquisition competitiveness is based on their relative demands. For example, CLM4CN [Thornton *et al.*, 2007] assumes that the plant and microbial nitrogen demands are satisfied simultaneously. Under nitrogen infertile conditions, all nitrogen demands in the system are down-regulated proportional to the individual demands and subject to available soil mineral nitrogen. This approach led to unrealistic diurnal cycles of gross primary production (GPP), with midday depressions in GPP occurring because of predicted diurnal depletion of the soil mineral nitrogen pool. Emergent impacts of this conceptualization of nutrient constraints on GPP resulted in poor predictions compared to observations, with smaller than observed plant C growth responses to N deposition

[*Thomas et al.*, 2013a] and larger than observed responses to N fertilization [*Thomas et al.*, 2013b]. Further, most biogeochemistry models not integrated in ESMs also adopt one of these approaches. For instance, Biome-BGC [*Running and Coughlan*, 1988], CENTURY [*Parton et al.*, 1988], CASA (Carnegie-Ames-Stanford Approach; [*Potter et al.*, 1993]) and the Terrestrial Ecosystem Model - TEM [*McGuire et al.*, 1992] assume that available nutrients preferentially satisfy the soil microbial immobilization demand.

We believe the two conceptualizations of competition used in ESMs substantially over-simplify competitive interactions between plants and microbes and lead to biases in carbon cycle predictions. To begin to address the problems with these simplified approaches, Tang and Riley (2013) showed that complex consumer-substrate networks can be represented with an approach (called Equilibrium Chemical Approximation (ECA) kinetics) that simultaneously resolves multiple demands for multiple substrates, and demonstrated that the approach was consistent with observed litter decomposition observations. ECA kinetics has also recently been applied to analyze the emergent temperature response of SOM decomposition, considering equilibrium, non-equilibrium, and enzyme temperature sensitivities and abiotic interactions with mineral surfaces [*Tang and Riley*, 2014]. We extend on that work here by presenting an implementation of ECA kinetics to represent competition for multiple soil nutrients in a multiple consumer environment. We note that this paper demonstrates a method to handle instantaneous competition in the complex soil-plant network, but a robust competition representation for climate-scale models will require representation of dynamic changes in plant allocation and plant composition.

150 The aim of this study is to provide a reliable nutrient competition approach
151 applicable for land models integrated in ESMs. However, before integration into an ESM,
152 the competition model needs to be carefully calibrated and independently tested against
153 observational data. This paper will therefore focus on model development and evaluation
154 at several tropical forest sites where observations are available. Our objectives are to: (1)
155 develop a soil biogeochemistry model with multiple nutrients (*i.e.*, NH_4^+ , NO_3^- , and PO_x
156 (represented as the sum of PO_4^{3-} , HPO_4^{2-} , and H_2PO_4^-)) and multiple nutrient consumers
157 (*i.e.*, decomposing microbes, plants, nitrifiers, denitrifiers, and mineral surfaces); (2)
158 represent nutrient competition with ECA kinetics [*Tang and Riley, 2013; Zhu and Riley,*
159 2015], accounting for substrate (multiple substrates for one consumer) and consumer
160 (multiple consumers competing for one substrate) effects; (3) constrain the model with *in*
161 *situ* observational datasets of soil carbon, nitrogen, and phosphorus dynamics using a
162 Markov Chain Monte Carlo (MCMC) approach; and (4) test model performance against
163 nitrogen and phosphorus fertilization studies.

2 Method

2.1 Model development

The Nutrient COMpetition model (N-COM) is designed as a soil biogeochemistry model (Figure 1) to simulate soil carbon decomposition, nitrogen and phosphorus transformations, abiotic interactions, and plant demands. Although our ultimate goal is to incorporate N-COM into a decomposition model that represents active microbial activity as the primary driver of decomposition, we start here by presenting the N-COM approach using a Century-like [Koven *et al.*, 2013; Parton *et al.*, 1988] structure, with additions to account for phosphorus dynamics. In our approach, we calculate potential immobilization using literature-derived parameters (*e.g.*, V_{MAX} , K_M) in a Michaelis-Menten (MM) kinetics framework. The potential immobilization is subsequently modified using the ECA competition method.

Five pools of soil organic Carbon (C), Nitrogen (N), and Phosphorus (P) are considered: Coarse Wood Debris (CWD), litter, fast Soil Organic Matter (SOM) pool, medium SOM pool, and slow SOM pool. Litter is further divided into three sub-groups: metabolic, cellulose, and lignin. The soil organic C, N, and P decomposition ($F_{C,j}^{dec}$, $F_{N,j}^{dec}$,

$F_{P,j}^{dec}$) follow first-order decay:

$$F_{C,j}^{dec} = k_j C_j r_\theta r_T \quad (1)$$

$$F_{N,j}^{dec} = k_j N_j r_\theta r_T \quad (2)$$

$$F_{P,j}^{dec} = k_j P_j r_\theta r_T \quad (3)$$

where k_j is the rate constant of soil organic matter decay (s^{-1}); C_j , N_j , and P_j are pool sizes ($g\ m^{-2}$) of carbon, nitrogen, and phosphorus, respectively (j from 1 to 7 represents the soil organic matter pools: CWD, metabolic litter, cellulose litter, lignin litter, fast

SOC, median SOC, slow SOC); r_T and r_θ (dimensionless) are soil temperature and moisture environmental regulators.

Decomposed carbon ($F_{C,i}^{dec}$) (upstream i^{th} pool) either (1) enters a downstream pool (j^{th}) or (2) is lost as CO_2 . Soil organic carbon (downstream j^{th} pool) temporal change is calculated as:

$$\frac{dC_j}{dt} = -F_{C,j}^{dec} + \sum_{i=1}^N F_{C,ij}^{move} \quad (4)$$

where $\sum_{i=1}^N F_{C,ij}^{move}$ is the summation of carbon fluxes that move from the upstream pool (i) to the downstream pool (j) due to the decomposition of upstream SOC. For each upstream carbon pool ($i = 1, 2, \dots, 7$), the fractions integrated into downstream pools ($j = 1, 2, \dots, 7$) is summarized in a 7 by 7 matrix f_{ij} (Table 2). The percentage of decomposed carbon that is respired as CO_2 is represented by g_i (Table 2). Simultaneously, soil organic N and P changes follow C decomposition:

$$\frac{dN_j}{dt} = -F_{N,j}^{dec} + \sum_{i=1}^N F_{N,ij}^{move} + \sum_{i=1}^N F_{NH4,ij}^{immob} + \sum_{i=1}^N F_{NO3,ij}^{immob} \quad (5)$$

$$\frac{dP_j}{dt} = -F_{P,j}^{dec} + \sum_{i=1}^N F_{P,ij}^{move} + \sum_{i=1}^N F_{P,ij}^{immob} \quad (6)$$

where $F_{N,ij}^{move}$ and $F_{P,ij}^{move}$ are fluxes of nitrogen and phosphorus moving from the upstream (i) to downstream (j) pools. $F_{NH4,ij}^{immob}$, $F_{NO3,ij}^{immob}$, and $F_{P,ij}^{immob}$ are immobilization fluxes of soil mineral nitrogen and phosphorus. $F_{N,j}^{dec}$ and $F_{P,j}^{dec}$ represent soil organic matter decomposition loss.

Equations (5) and (6) state that changes in the j^{th} organic N or P pool are the summation of three terms: (1) organic N and P lost during soil organic matter mineralization ($-F_{N,j}^{dec}$ and $-F_{P,j}^{dec}$); (2) a fraction of the i^{th} organic N or P pool (upstream) enters into the j^{th} pool (downstream) ($F_{N,ij}^{move}$ and $F_{P,ij}^{move}$); and (3) soil microbial immobilization ($F_{NH_4,ij}^{immob}$, $F_{NO_3,ij}^{immob}$, and $F_{P,ij}^{immob}$). Immobilization occurs only when the newly entering organic N is insufficient to sustain the soil C:N (or C:P) ratio (more details described in Appendix A).

The inorganic nitrogen pools (NH_4^+ and NO_3^- (Eqn. 7 -8)) are altered by production (organic N mobilized by microbes), consumption (uptake by plants and microbes, gaseous or aqueous losses), and transformation (nitrification and denitrification). Inorganic P (PO_x) is assumed to be either taken up by plants and decomposing microbes or adsorbed to mineral surfaces (Eqn. 9). Plants utilize all forms of phosphate (*e.g.*, PO_4^{3-} , HPO_4^{2-} , and $H_2PO_4^-$), but for simplicity we use the symbol PO_x to represent the sum of all possible phosphate forms throughout the paper.

$$\frac{d[NH_4]}{dt} = \sum_{j=1}^N \sum_{i=1}^N F_{NH_4,ij}^{mob} - F_{NH_4}^{nit} - F_{NH_4}^{plant} - F_{NH_4}^{immob} + F^{BNF} + F_{NH_4}^{dep} \quad (7)$$

$$\frac{d[NO_3]}{dt} = -F_{NO_3}^{den} + (1 - f^{N_2O})F_{NH_4}^{nit} - F_{NO_3}^{plant} - F_{NO_3}^{immob} - F_{NO_3}^{leach} + F_{NO_3}^{dep} \quad (8)$$

$$\frac{d[PO_x]}{dt} = \sum_{j=1}^N \sum_{i=1}^N F_{P,ij}^{mob} - F_P^{plant} - F_P^{immob} - F_P^{surf} - F_P^{leach} + F^{weather} \quad (9)$$

where $F_{NH_4,ij}^{mob}$ and $F_{P,ij}^{mob}$ are gross mineralization rates for nitrogen and phosphorus. $F_{NH_4}^{nit}$ is the nitrification flux, part of which is lost through a gaseous pathway (f^{N_2O}) and the rest is incorporated into the NO_3^- pool. $F_{NO_3}^{den}$ is the denitrification flux, which transforms nitrate to N_2O and N_2 which then leave the soil system. Plant uptake of soil NH_4^+ , NO_3^- ,

and PO_x are represented as $F_{NH_4}^{plant}$, $F_{NO_3}^{plant}$, and F_P^{plant} , respectively. Soil decomposing microbial immobilization of soil NH_4^+ , NO_3^- , and PO_x are represented as $F_{NH_4}^{immob}$, $F_{NO_3}^{immob}$, and F_P^{immob} , $F_{NO_3}^{leach}$, and F_P^{leach} are leaching losses of soil NO_3^- and PO_x . External inputs into soil inorganic N pools include atmospheric ammonia deposition ($F_{NH_4}^{dep}$), atmospheric nitrate deposition ($F_{NO_3}^{dep}$), and biological nitrogen fixation (F^{BNF}). External sources of phosphate come from parent material weathering ($F^{weather}$).

Finally, the dynamics of sorbed P (P_s), occluded P (P_o), and parent material P (P_p) are modeled as:

$$\frac{d[P_s]}{dt} = F_P^{surf} - F_P^{occl} \quad (10)$$

$$\frac{d[P_o]}{dt} = F_P^{occl} \quad (11)$$

$$\frac{d[P_p]}{dt} = -F^{weather} + F_P^{dep} \quad (12)$$

where the pool of sorbed P is balanced by the adsorption flux (F_P^{surf}) and occlusion flux (F_P^{occl}). Parent material is lost by weathering ($F^{weather}$) and is slowly replenished by external atmospheric phosphorus inputs (F_P^{dep} , such as dust). More detailed information on the modeled C, N, and P fluxes is documented in Appendix A.

2.2 Multiple-consumer-multiple-resource competition network

The soil biogeochemistry model presented in **section 2.1** has multiple potential nutrient consumers (plants, SOM decomposing microbes, nitrifiers, denitrifiers, mineral surfaces) and multiple soil nutrients (NH_4^+ , NO_3^- , PO_x). The consumer-resource network is summarized in Table 1. As in many land BGC models (CLM, Century, *etc.*), we have

not explicitly included the mineral surface adsorptions of NH_4^+ and NO_3^- , since we assume ammonia is quickly protected by mineral surfaces from leaching (no leaching term in Eqn. 7) but then released for plant and microbial uptake when the biotic demand arises. An improved treatment of these dynamics would necessitate a prognostic model for pH, which is beyond the scope of this analysis. Unlike sorbed P (which can be occluded), there is no further abiotic loss of sorbed ammonia. Therefore, the free ammonia pool is interpreted in the current model structure as a potential free ammonia pool (free + sorbed).

Competition between different consumers in acquiring different resources is summarized in Table 1. Each consumer-substrate competition reaction is represented by:



The enzyme (E : e.g., *nutrient carrier enzyme produced by plants and microbes*) and substrate (S : e.g., NH_4^+ , NO_3^-) reaction (reversible reaction) forms a substrate-enzyme complex (SE). The following irreversible reaction leads to product (P : meaning *the nutrients has been taken up*) and releases enzyme (E) back into soil media. For the whole complex reaction network, nutrient uptakes are formulated as:

$$F_{\text{NH}_4}^{\text{plant}} = k_{\text{NH}_4}^{\text{plant}} \cdot \frac{[\text{NH}_4] \cdot [E_N^{\text{plant}}]}{KM_{\text{NH}_4}^{\text{plant}} \left(1 + \frac{[\text{NH}_4]}{KM_{\text{NH}_4}^{\text{plant}}} + \frac{[\text{NO}_3]}{KM_{\text{NO}_3}^{\text{plant}}} + \frac{[E_N^{\text{plant}}]}{KM_{\text{NH}_4}^{\text{plant}}} + \frac{[E_N^{\text{mic}}]}{KM_{\text{NH}_4}^{\text{mic}}} + \frac{[E_N^{\text{nit}}]}{KM_{\text{NH}_4}^{\text{nit}}} \right)} \quad (14)$$

$$F_{\text{NH}_4}^{\text{immob}} = k_{\text{NH}_4}^{\text{immob}} \cdot \frac{[\text{NH}_4] \cdot [E_N^{\text{mic}}]}{KM_{\text{NH}_4}^{\text{mic}} \left(1 + \frac{[\text{NH}_4]}{KM_{\text{NH}_4}^{\text{mic}}} + \frac{[\text{NO}_3]}{KM_{\text{NO}_3}^{\text{mic}}} + \frac{[E_N^{\text{plant}}]}{KM_{\text{NH}_4}^{\text{plant}}} + \frac{[E_N^{\text{mic}}]}{KM_{\text{NH}_4}^{\text{mic}}} + \frac{[E_N^{\text{nit}}]}{KM_{\text{NH}_4}^{\text{nit}}} \right)} \quad (15)$$

$$F_{\text{NH}_4}^{\text{nit}} = k_{\text{NH}_4}^{\text{nit}} \cdot \frac{[\text{NH}_4] \cdot [E_{\text{NH}_4}^{\text{nit}}]}{KM_{\text{NH}_4}^{\text{nit}} \left(1 + \frac{[\text{NH}_4]}{KM_{\text{NH}_4}^{\text{nit}}} + \frac{[E_N^{\text{plant}}]}{KM_{\text{NH}_4}^{\text{plant}}} + \frac{[E_N^{\text{mic}}]}{KM_{\text{NH}_4}^{\text{mic}}} + \frac{[E_N^{\text{nit}}]}{KM_{\text{NH}_4}^{\text{nit}}} \right)} \quad (16)$$

$$265 \quad F_{NO_3}^{plant} = k_{NO_3}^{plant} \cdot \frac{[NO_3] \cdot [E_N^{plant}]}{KM_{NO_3}^{plant} \left(1 + \frac{[NH_4]}{KM_{NH_4}^{plant}} + \frac{[NO_3]}{KM_{NO_3}^{plant}} + \frac{[E_N^{plant}]}{KM_{NO_3}^{plant}} + \frac{[E_N^{mic}]}{KM_{NO_3}^{mic}} + \frac{[E_N^{den}]}{KM_{NO_3}^{den}}\right)} \quad (17)$$

$$266 \quad F_{NO_3}^{immob} = k_{NO_3}^{immob} \cdot \frac{[NO_3] \cdot [E_N^{mic}]}{KM_{NO_3}^{mic} \left(1 + \frac{[NH_4]}{KM_{NH_4}^{mic}} + \frac{[NO_3]}{KM_{NO_3}^{mic}} + \frac{[E_N^{plant}]}{KM_{NO_3}^{plant}} + \frac{[E_N^{mic}]}{KM_{NO_3}^{mic}} + \frac{[E_N^{den}]}{KM_{NO_3}^{den}}\right)} \quad (18)$$

$$267 \quad F_{NO_3}^{den} = k_{NO_3}^{den} \cdot \frac{[NO_3] \cdot [E_{NO_3}^{den}]}{KM_{NL3}^{den} \left(1 + \frac{[NO_3]}{KM_{NO_3}^{den}} + \frac{[E_N^{plant}]}{KM_{NO_3}^{plant}} + \frac{[E_N^{mic}]}{KM_{NO_3}^{mic}} + \frac{[E_N^{den}]}{KM_{NO_3}^{den}}\right)} \quad (19)$$

$$268 \quad F_p^{plant} = k_p^{plant} \cdot \frac{[PO_x] \cdot [E_p^{plant}]}{KM_p^{plant} \left(1 + \frac{[PO_x]}{KM_p^{plant}} + \frac{[E_p^{plant}]}{KM_p^{plant}} + \frac{[E_p^{mic}]}{KM_p^{mic}} + \frac{[E_p^{surf}]}{KM_p^{surf}}\right)} \quad (20)$$

$$269 \quad F_p^{mic} = k_p^{mic} \cdot \frac{[PO_x] \cdot [E_p^{mic}]}{KM_p^{mic} \left(1 + \frac{[PO_x]}{KM_p^{mic}} + \frac{[E_p^{plant}]}{KM_p^{plant}} + \frac{[E_p^{mic}]}{KM_p^{mic}} + \frac{[E_p^{surf}]}{KM_p^{surf}}\right)} \quad (21)$$

$$270 \quad F_p^{surf} = k_p^{surf} \cdot \frac{[PO_x] \cdot [E_p^{mic}]}{KM_p^{surf} \left(1 + \frac{[PO_x]}{KM_p^{surf}} + \frac{[E_p^{plant}]}{KM_p^{plant}} + \frac{[E_p^{mic}]}{KM_p^{mic}} + \frac{[E_p^{surf}]}{KM_p^{surf}}\right)} \quad (22)$$

271 where F represent the nutrient uptake fluxes and k is the base reaction rate that enzyme-
 272 substrate complex forms product (k_2^+ in Eqn. 13). $[E]$ and KM denote enzyme abundance
 273 and half saturation constants (substrate-enzyme affinity). Superscripts and subscripts
 274 refer to consumers and substrates. These equations account for the effect of (1) multiple
 275 substrates (e.g., NH_4^+ and NO_3^-) sharing one consumer, which inhibits the effective
 276 binding between any specific substrate and the consumer (terms ⁽¹⁾ and ⁽²⁾ in Eqn. 14) and
 277 (2) multiple consumers (e.g., plants, decomposing microbes, and nitrifiers) sharing one

substrate (*e.g.*, NH_4^+), which lowers the probability of effective binding between any consumer and NH_4^+ (terms ⁽³⁾, ⁽⁴⁾, and ⁽⁵⁾ in Eqn. 14).

For our reaction network (Eqn. 13 – 22), we assume that: (1) plant roots and decomposing microbes possess two types of nutrient carrier enzymes (nutrient transporters). One is for nitrogen (NH_4^+ and NO_3^- ; E_N^{plant} , E_N^{mic}), and the other is for phosphorus, including different forms of phosphate (E_P^{plant} , E_P^{mic}). (2) Nutrient carrier enzyme abundance is scaled with biomass (fine root or microbial biomass). Scaling factors are 0.0000125 (for plants) and 0.05 (for decomposing microbes) (Table 2). (3) Mineral surface “effective enzyme” abundance (E_p^{surf}) is approximated by $VMAX_p^{surf} - [SP]$. (4) Nitrifiers and denitrifiers are not explicitly simulated, therefore we assume that their biomass and associated nutrient transporter abundance are fixed (E_N^{nit} , E_N^{denit}).

For simplicity, we group the “decomposing microbes/nitrifier/denitrifier/mineral surface nutrient carrier enzyme [E]” and their “base reaction rate k ” into one single variable “ $VMAX$ ” (see Appendix B for full derivation). Furthermore, we defined “potential rates (potential immobilization, nitrification, denitrification, adsorption rates)” and used them as proxies of “ $VMAX$ ”. Therefore, Eqn. 15, 16, 18, 19, 21, 22 become:

$$F_{NH_4}^{immob} = F_{NH_4}^{immob,pot} \cdot \frac{[NH_4]}{KM_{NH_4}^{mic} \left(1 + \frac{[NH_4]}{KM_{NH_4}^{mic}} + \frac{[NO_3]}{KM_{NO_3}^{mic}} + \frac{[E_N^{plant}]}{KM_{NH_4}^{plant}} + \frac{[E_N^{mic}]}{KM_{NH_4}^{mic}} + \frac{[E_N^{nit}]}{KM_{NH_4}^{nit}} \right)} \quad (23)$$

$$F_{NH_4}^{nit} = F_{NH_4}^{nit,pot} \cdot \frac{[NH_4]}{KM_{NH_4}^{nit} \left(1 + \frac{[NH_4]}{KM_{NH_4}^{nit}} + \frac{[E_N^{plant}]}{KM_{NH_4}^{plant}} + \frac{[E_N^{mic}]}{KM_{NH_4}^{mic}} + \frac{[E_N^{nit}]}{KM_{NH_4}^{nit}} \right)} \quad (24)$$

$$297 \quad F_{NO3}^{immob} = F_{NO3}^{immob,pot} \cdot \frac{[NO3]}{KM_{NO3}^{mic} \left(1 + \frac{[NH4]}{KM_{NH4}^{mic}} + \frac{[NO3]}{KM_{NO3}^{mic}} + \frac{[E_N^{plant}]}{KM_{NO3}^{plant}} + \frac{[E_N^{mic}]}{KM_{NO3}^{mic}} + \frac{[E_N^{den}]}{KM_{NO3}^{den}}\right)} \quad (25)$$

$$298 \quad F_{NO3}^{den} = F_{NO3}^{den,pot} \cdot \frac{[NO3]}{KM_{NL3}^{den} \left(1 + \frac{[NO3]}{KM_{NO3}^{den}} + \frac{[E_N^{plant}]}{KM_{NO3}^{plant}} + \frac{[E_N^{mic}]}{KM_{NO3}^{mic}} + \frac{[E_N^{den}]}{KM_{NO3}^{den}}\right)} \quad (26)$$

$$299 \quad F_P^{mic} = F_P^{immob,pot} \cdot \frac{[PO_x]}{KM_P^{mic} \left(1 + \frac{[PO_x]}{KM_P^{mic}} + \frac{[E_P^{plant}]}{KM_P^{plant}} + \frac{[E_P^{mic}]}{KM_P^{mic}} + \frac{[E_P^{surf}]}{KM_P^{surf}}\right)} \quad (27)$$

$$300 \quad F_P^{surf} = F_P^{surf,pot} \cdot \frac{[PO_x]}{KM_P^{surf} \left(1 + \frac{[PO_x]}{KM_P^{surf}} + \frac{[E_P^{plant}]}{KM_P^{plant}} + \frac{[E_P^{mic}]}{KM_P^{mic}} + \frac{[E_P^{surf}]}{KM_P^{surf}}\right)} \quad (28)$$

301 In this case, the potential rates are treated as maximum reaction rates ($VMAX$),
 302 because they are calculated without nutrient constraints or biotic and abiotic interactions.
 303 For example, potential P immobilization rate ($F_P^{immob,pot}$) is based on the total phosphorus
 304 demand that can perfectly maintain the soil CP stoichiometry during soil organic matter
 305 decomposition (Eqn. A9). This potential immobilization rate represents the maximum
 306 phosphorus influx that the soil could take up at that moment. The maximum adsorption
 307 rate ($F_P^{surf,pot}$) is the time derivative of the Langmuir equation (Eqn. A12), which is a
 308 theoretically maximal adsorption rate excluding all other biotic and abiotic interactions.
 309 The potential rates ($VMAX$) are updated by the model rather than calibrated, except for
 310 $VMAX_P^{surf}$. $VMAX_P^{surf}$ denotes the maximum adsorption capacity (not maximum
 311 adsorption rate), which affects the potential adsorption rate ($F_P^{surf,pot}$).

312 The model is run on an hourly time step, initialized with state variables and
 313 critical parameters (Table 2). Since the model is designed to be a component of the

Community and ACME Land Models (CLM, ALM; which are essentially equivalent at this time), we used CLM4.5 site-level simulations to acquire temporally-resolved: (1) soil temperature factors on decomposition (r_T); (2) soil moisture factors on decomposition (r_θ); (3) the anoxic fraction of soil pores (f^{anox} in Appendix Eqn. A10-11); (4) annual NPP (NPP_{annual} in Appendix Eqn. A13); (5) NH_4^+ deposition ($F_{\text{NH}_4}^{dep}$); (6) NO_3^- deposition ($F_{\text{NO}_3}^{dep}$); and (7) hydrologic discharge (Q_{dis} in Appendix Eqn. A14). External inputs of mineral phosphorus are derived from Mahowald *et al.*, [2005, 2008].

2.3 Model parameterization and sensitivity analysis

We constrained model parameters and performed sensitivity analyses using a suite of observations distinct from the observations we used subsequently to test the model against the N and P manipulation experiments. Because tropical systems can be either nitrogen or phosphorous limited (or both) [Elser *et al.*, 2007; Vitousek *et al.*, 2010], we chose observations from a tropical forest site to constrain the N and P competition in our model (Tapajos National Forest, Para, Brazil (Table 3)).

In the parameter estimation procedure, several data streams are assimilated into the N-COM model, including measurements of soil NH_4^+ concentrations, soil free phosphate concentrations, sorbed phosphate concentrations, and N_2O and CO_2 flux measurements. The datasets are summarized in Table 3 and cover a wide range of N and P biogeochemistry dynamics. A set of model parameters is selected for calibration (Table 4), which comprise nutrient competition kinetics parameters (k and KM) as well as the fast soil carbon turnover time ($TURN_{SOM}$). Because we had only a short-term CO_2 respiration flux record, we were unable to calibrate the longer turnover time parameters. However, since we test the posterior model against short-term fertilization responses, this

omission will not affect our evaluation. Longer records from eddy covariance flux towers and ^{14}C soil measurements are required to constrain the longer turnover time pool values.

We employed the Markov Chain Monte Carlo (MCMC) approach [Ricciuto *et al.*, 2008] to assimilate the observations into N-COM. MCMC directly draws samples from a pre-defined parameter space and tries to minimize a pre-defined cost function:

$$J = (M(\theta) - D)^T R^{-1} (M(\theta) - D) \quad (29)$$

where $M(\theta)$ and D are vectors of model outputs and observations including time series of different simulated variables (*e.g.*, soil CO_2 and N_2O effluxes and soil concentrations of NH_4^+ , free PO_x , and sorbed PO_x); θ is a vector of model parameters (θ_i); and i from 1 to 20 represents the parameters that are calibrated (Table 4). R^{-1} is the inverse of data error covariance matrix. We assumed that diagonal elements are 40% of observed value and off-diagonal elements are zeros. We further assumed that the prior parameter follows a lognormal distribution. μ and σ were 0.91 and 0.95 of their initial values, respectively (Table 4). We then ran MCMC to sample 50,000 parameter pairs, which in our simulations was sufficient to ensure thorough convergence (Fig. A1). The second half of the samples was used to calculate the posterior parameter space by fitting to a Gaussian distribution. The posterior model parameters are reported in term of means and standard deviations. The Uncertainty Reduction (UR) is defined as:

$$UR = \left(1 - \frac{\sigma_{posterior}}{\sigma_{prior}}\right) \cdot 100\% \quad (30)$$

where σ_{prior} is prior parameter uncertainty, which is 95% of the parameter initial value.

$\sigma_{posterior}$ is posterior parameter uncertainty, which is calculated by fitting the posterior model parameters to a Gaussian distribution. Uncertainty Reduction is a useful metric

[Zhu and Zhuang, 2014], because it quantitatively reveals the reduction in the range of a particular parameter after calibration with MCMC. It does not indicate that the parameter itself is more consistent with observed values of the parameter. UR is sensitive to the assumption of prior uncertainty range. A large value of UR implies a more robust posterior model.

In addition, we conducted a sensitivity study to identify the dominant controlling factors regulating nutrient competition in N-COM. Three scenarios were considered: (1) baseline climate and soil conditions; (2) elevated soil temperature (by 5 °C); and (3) elevated soil moisture (by 50%). SOBOL sampling [Pappas *et al.*, 2013], a global sensitivity technique, is employed to calculate the sensitivities of output variables with respect to various inputs:

$$S_i = \frac{VAR_{p_i}(E_{p_{-i}}(Y|p_i))}{VAR(Y)} \quad (31)$$

where S_i is the first order sensitivity index of the i^{th} parameter and ranges from 0 to 1. By comparing the values of S_i , we were able to evaluate which processes were relatively more important in affecting nutrient competition. Y represents the model outputs of plant NH_4^+ , NO_3^- , or PO_x uptake; p_i is the target parameter; p_{-i} denotes all parameters that are associated with nutrient competition except the target parameter; and $VAR(.)$ and $E(.)$ represent variance and mean, respectively.

2.4 Model application

After calibration, we applied the N-COM model to several tropical forest nutrient fertilization studies not included in the calibration dataset, where isotopically labeled nitrogen or phosphorous fertilizer was injected into the soil. The fertilization experiments

measured the fate of added nutrients; for example, identifying the fraction of added N or P that goes into the plant, is immobilized by microbes, or is stabilized by mineral surfaces. These measurements offer an effective baseline to test whether the N-COM model captures short-term nutrient competition.

Because we have focused in this paper on applications in tropical forests, we choose three tropical forest fertilization experiments with (1) PO_4^{3-} ; (2) NH_4^+ ; and (3) NO_3^- additions (Table 5). The PO_4^{3-} fertilization experiment [Olander and Vitousek, 2005] was conducted in three Hawaiian tropical forests along a soil chronosequence (300, 20000, and 4100000 year old soils) that were fertilized with $10 \mu\text{g g}^{-1} {}^{32}\text{PO}_4^{3-}$, respectively, and microbial demand versus soil sorption was measured. We did not evaluate the role of plants in phosphorus competition for the Hawaii sites, since plant phosphorus uptake was not measured in those field studies. Our model discriminates the Hawaii sites along the chronosequence by setting distinct initial pool sizes (derived from [Olander and Vitousek, 2004; Olander and Vitousek, 2005]) of soil organic carbon, nitrogen and phosphorus, and soil parent material phosphorus.

We also used measurements from NH_4^+ and NO_3^- fertilization studies located at the Luquillo tropical forest in Puerto Rico [Templer *et al.*, 2008]. In that study, $4.6 \mu\text{g g}^{-1} {}^{15}\text{NH}_4^+$ was added into the highly weathered tropical forest soil and the consumption of ${}^{15}\text{NH}_4^+$ by plant roots, decomposing microbes, and nitrifiers were measured. In the same study, $0.92 \mu\text{g g}^{-1} {}^{15}\text{NO}_3^-$ was added to the soil and the plant uptake and microbial immobilization was measured. The measurements were made 24 or 48 hours after the fertilizers were added.

For the model scenarios, we (1) spun up the N-COM model for 100 years; (2) perturbed the soil nutrient pool by the same amount as the fertilization; (3) ran the model for 24 or 48 hours and calculated how much of the added nutrients were absorbed by plants, microbes, or mineral surfaces; and (4) compared our model simulations with the observed data to assess model predictability. The 100-year spin up simulation aimed at eliminating the effects of imposed initial inorganic pool sizes on fertilization experiments, rather than accumulating soil organic matter in the system, since we initialized the soil organic carbon pools from CLM4.5 steady state predictions.

3. Results and discussion

3.1 Posterior model parameters

Our best estimates (second half of the MCMC chain) of the selected model parameters based on the observations at the Tapajos National Forest, Para, Brazil are shown in Figure 2. We found that posterior parameter samples were not heavily tailed and they generally follow Gaussian distributions (Figure A2). In order to quantitatively compare the posterior parameter distributions with prior distributions, we fit parameter samples to a Gaussian distribution and estimated its means and standard deviations (Table 4).

Even though the posterior mean was improved, the uncertainty of the posterior model may still be relatively large. In other words, a prognostic prediction based on these posterior parameters could be relatively uncertain [Scholze *et al.*, 2007], due to large uncertainty associated with the posterior parameters. Therefore, we calculated the Uncertainty Reduction (*UR*) to evaluate model improvement in terms of posterior

uncertainty. We found that parameters' uncertainties were reduced by 13%~98%. This calculation might either overestimate or underestimate the UR , due to the fact that the posterior parameters did not strictly follow Gaussian distributions. But the actual UR should not be far from our estimates, because the posterior samples were not widely spread across the potential parameter space (Figure 2). The least constrained parameter was $k_{NO_3}^{plant}$ (reaction rate of plant nitrogen carrier enzyme with NO_3^- substrate). Two other NO_3^- dynamics related parameters were also not well constrained: UR of $KM_{NO_3}^{mic}$ (half-saturation constant for decomposing microbe NO_3^- immobilization) and $KM_{NO_3}^{den}$ (half-saturation constant for denitrifier NO_3^- consumption) were only 64% and 67%, respectively. Compared with NH_4^+ or PO_4 competition related parameters, we concluded that parameters associated with NO_3^- competition were the least constrained in the model. This was primarily due to the lack of NO_3^- pool size data, and secondarily due to the fact that NO_3^- was not the major nitrogen source for plant or decomposing microbes.

We re-organize the right hand sides of Eqns. 14 – 22 and define those fraction terms as relative competitiveness parameter (ECA); for example for plant NH_4^+ uptake:

$$F_{NH_4}^{plant} = k_{NH_4}^{plant} \cdot ECA_{NH_4}^{plant} \quad (32)$$

$$ECA_{NH_4}^{plant} = \frac{[NH_4] \cdot [E_N^{plant}]}{KM_{NH_4}^{plant} \left(1 + \frac{[NH_4]}{KM_{NH_4}^{plant}} + \frac{[NO_3]}{KM_{NO_3}^{plant}} + \frac{[E_N^{plant}]}{KM_{NH_4}^{plant}} + \frac{[E_N^{mic}]}{KM_{NH_4}^{mic}} + \frac{[E_N^{nit}]}{KM_{NH_4}^{nit}} \right)} \quad (33)$$

Other “consumer-substrate reactions” have similar forms. Under a nutrient abundant situation (*e.g.*, fertilized agriculture ecosystem), the relative competitiveness of each consumer (ECA) is dominated by its specific enzyme abundance ($[E]$). Under such conditions, substrate affinity is no longer a controlling factor. In contrast, under nutrient

limited conditions (*e.g.*, natural ecosystem), ECA is dominated by the specific enzyme abundance as well as the substrate affinity ($[E]/KM$). Therefore, consumers could either enable an alternative high affinity nutrient transporter system (low KM) or exudate more enzyme to enhance competitiveness. For example, it has been shown that root spatial occupation (C_{root}) determines plant's competitiveness when low soil nutrient diffusivity is limiting nutrient supply [Raynaud and Leadley, 2004]. Consistently, our results highlighted the dominant role of nutrient carrier enzyme abundance (E proportional to C_{root}) in controlling competition. If we further assumed that plants, decomposing microbes, and nitrifiers enzyme abundances were approximately equal, we will have that the relative their competitiveness in acquiring NH_4^+ was about 4:10:9 ($1 / KM_{NH_4}^{plant} : 1 / KM_{NH_4}^{mic} : 1 / KM_{NH_4}^{nit}$). However, such results could not be easily generalized to other ecosystems, because they heavily relied on the traits (affinity) of specific competitors. For a different ecosystem, those traits would be drastically different due to the change of, *e.g.*, plant species composition and microbial community structure. Even for the same ecosystem, those traits could be highly heterogeneous. For example, the community structure of decomposing microbes could be different in rhizosphere and bulk soil (with different KM). However, in this work we assumed a well-mixed environment (one soil column), in order to be consistent with large-scale ecosystem models.

Our modeling framework highlights the important concept that “competitiveness” is a dynamic property of the competition network, and more importantly that it is linked to competitor functional traits (affinity and nutrient carrier enzyme abundance). This concept is in contrast to the prevailing assumption underlying all major large-scale ecosystem models, which either assume “relative demand competitiveness for different

nutrient consumers” [Thornton *et al.*, 2007] or “soil microbes outcompete plants” [McGuire *et al.*, 1992; Parton *et al.*, 1988]. Imposing such pre-defined orders of competitiveness neglects the diversity of nutrient competitors (plants and microbes) and their differences in nutrient uptake capacity expressed by relevant functional traits. Our model framework offers a theoretically consistent approach to account for the diversity of nutrient competition in different competitor networks.

3.2 Model sensitivity analysis

Through sensitivity analysis, we separately investigated the factors controlling plant NH_4^+ , NO_3^- , and PO_x competition (Figure 3). Each sensitivity analysis consisted of three scenarios: (1) normal conditions (control); (2) elevated soil T ($+T_s$); and (3) elevated soil moisture ($+\theta$). The sensitivity indicates that nutrient competition is mostly regulated by internal competitor kinetics rather than external environmental conditions (*e.g.*, T_s , θ). The environment affects the nutrient competition primarily through altering the nutrient abundance. Enhanced soil temperature and soil moisture accelerated soil organic carbon turnover, thereby releasing more inorganic nutrient into the soil (gross mineralization). However, the impacts on plant nutrient uptake are limited (Figure 3) because the enhanced soil organic matter decay also requires higher immobilization fluxes to sustain the soil organic matter CNP stoichiometry. The enhancement of net mineralization would be limited, and therefore would not change soil nutrient status dramatically.

3.3 Posterior model performance

The prior and posterior models were compared against observational datasets of pool sizes of soil free phosphate, sorbed phosphate, and NH_4^+ , CO_2 efflux, and N_2O

efflux (Figure 4). We note that although we attempted to acquire as many datasets that contained these five observations as possible, more observations in tropical ecosystems would clearly improve the posterior parameter estimates. The prior model predicted an increasing trend of soil free PO_x , which resulted from underestimates of plant P uptake (by underestimating of k_p^{plant}) and soil microbial P immobilization (by overestimating KM_p^{mic}). The posterior model captured the seasonal dynamics of soil free PO_x reasonably well: increases during the wet season and gradual decreasing during the dry season (August to November). The prior model also largely underestimated the seasonal variability of nitrogen dynamics and underestimated the NH_4^+ pool size due to overestimation of plant NH_4^+ uptake ($k_{NH_4}^{plant}$). In addition, it also underestimated the denitrification N_2O emissions, because of an underestimation of NH_4^+ to NO_3^- transformation rate (k_{nit}). Consequently, there was not enough NO_3^- substrate to react with denitrifiers and release N_2O . The posterior model, however, accurately reproduced the seasonal dynamics of both NH_4^+ pool sizes and soil N_2O emissions. There were small differences between the prior and posterior model predictions of soil CO_2 emissions. The CO_2 and N_2O effluxes were more frequently observed at Tapajos National Forest during 1999 to 2001, compared with phosphorus data. Most of the measurements were collected during the wet season. Therefore the modeled CO_2 and N_2O emissions were largely improved by assimilating these datasets.

The posterior model performance implies that after assimilating multiple datasets, our model predictions were improved over the prior model. However, it is clear that more observations of the metrics applied in our MCMC approach would benefit the posterior model. Unfortunately, because of our focus on tropical sites, we were unable to acquire

more datasets that had the full suite of measurements required. Datasets of soil nutrient pool sizes (*e.g.*, NO_3^-) and CO_2 and N_2O effluxes with higher frequency sampling would significantly benefit the model uncertainty reduction.

3.4 Model testing against nitrogen and phosphorus fertilization studies

To test the posterior N-COM model, we conducted short-term numerical competition experiments (24-hour or 48-hour simulations) by manually imposing an input flux into nutrient pools equivalent to the N and P fertilization experiments described above and in Table 5. The simulated results were compared with observations from the field manipulations.

In the P addition experiments across the Hawaiian chronosequence, the partitioning of phosphate between microbes and mineral surfaces was well represented by the N-COM model in the intermediate (20K yr) and old (4.1M yr) sites (Figures 5b and 5c), with no significant differences between model predictions and observations. In the youngest Hawaiian site (300 yr; Figure 5a), the relative partitioning was correctly simulated, but the predicted PO_4^{3-} magnitudes were lower than observations. Our simulations indicated that at the young soil site the added P exceeded microbial demand, resulting in lower predicted microbial P uptake than observed. This discrepancy reflected a possible deficiency of first-order SOC decay models (as we used here), which implicitly treat microbes as a part of soil organic matter. Since microbial nutrient immobilization is strictly regulated by the SOC turnover rate in this type of model, external nutrient inputs will no longer affect microbial nutrient uptake if the inputs exceed potential microbial demand. We therefore believe that explicit Microbe-Enzyme models might be able to better explain the strong microbe PO_4^{3-} uptake signal observed at the young Hawaii

fertilization experiment site. Microbial models explicitly simulate the dynamics of microbial biomass, which might be able to capture the expected rapid growth of microbial communities under conditions of improved substrate quality [Kaspari *et al.*, 2008; Wieder *et al.*, 2009].

In the Puerto Rican Luquillo forest nitrogen addition experiments, partitioning of added ammonium between plants and heterotrophic bacteria was well captured by the N-COM model, with no significant differences between model predictions and observations (Figure 5d). However, the model underestimated nitrifier NH_4^+ uptake. NO_3^- competition in this site was also relatively accurately predicted (Figure 5e), although the measurements did not include denitrification. Model estimates of plant NO_3^- uptake and microbial NO_3^- immobilization were consistent with the observed ranges, but we highlight the large observational uncertainties, particularly for microbial NO_3^- uptake.

In the pseudo-first-order decomposition model we applied here to demonstrate the ECA competition methodology, the soil organic matter C/N/P ratio also limited microbial N/P uptake. For this type of decomposition model, stoichiometric differences between soil organic matter and microbes are not dynamically simulated. Such a simplification of soil and microbial stoichiometry favors large spatial scale model structures over long temporal periods, but hampers prediction of microbial short-term responses to N/P fertilization. For example, the observed difference between microbial and soil C/P ratios can be as large as 6-fold [Mooshammer *et al.*, 2014; Xu *et al.*, 2013]. Were that the case in the observations we applied, the potential soil P demand calculated based on a fixed soil organic matter C/P ratio could be only 17% of that based on microbial C/P ratio.

3.5 Implications of ECA competition treatment

Terrestrial ecosystem growth and function are continuously altered by climate (e.g., warming, drought; [Chaves *et al.*, 2003; Springate and Kover, 2014]), external nutrient inputs (e.g., N deposition; [Matson *et al.*, 2002; Matson *et al.*, 1999]), and atmospheric composition (e.g., CO₂ concentration; [Norby *et al.*, 2010; Oren *et al.*, 2001; Reich *et al.*, 2006]). Improved understanding of the underlying mechanisms regulating ecosystem responses to environmental changes has been obtained through *in situ* level to large-scale and long-term manipulation experiments. For example, decade-long Free-Air Carbon Dioxide Enrichment (FACE) experiments have revealed that nitrogen limitation diminished the CO₂ fertilization effect of forests [Norby *et al.*, 2010] and grasslands [Reich and Hobbie, 2013] ecosystems. However, fewer efforts have been made towards incorporating the observed process-level knowledge into Earth System Models (ESMs). Therefore, a major uncertainty that has limited the predictability of ESMs has been the incomplete representation of soil nutrient dynamics [Zaehle *et al.*, 2014]. Even though new soil nutrient cycle paradigms were proposed during recent decades [Korsaeth *et al.*, 2001; Schimel and Bennett, 2004], they were restricted to either conceptual models or only applied to explain laboratory experiments.

Many large-scale terrestrial biogeochemistry models (e.g., O-CN, CASA, TEM) have adopted the classical paradigm that microbes decompose soil organic matter and release NH₄⁺ as a “waste” product [Waksman, 1931]. The rate of this process is defined as “net N mineralization”, and is adopted as a “measure” of plant available inorganic N [Schimel and Bennett, 2004]. This classical paradigm overlooked the fact that “net N mineralization” actually comprised two individual processes - gross N mineralization and microbial N immobilization. Implicitly, the classical paradigm assumes that the microbes

have priority to assimilate as much of the available nutrient pool as possible. Soil nutrients were only available for plant uptake if there were not enough free energy materials (*e.g.*, dissolved soil organic carbon) to support microbial metabolism. As a result, soil microbes were considered “victors” in the short-term nutrient competition. Some other large-scale terrestrial biogeochemistry models (*e.g.*, CLM4CN), simplify the concept of nutrient competition differently. They calculate the plant N uptake and soil N immobilization separately; and then down-regulate the two fluxes according to the soil mineral N availability. As a result, plant and soil microbe competitiveness for nutrients is determined by their relative demand.

Climate-scale land models have over-simplified or ignored competition between plants, microbes, and abiotic mechanisms. In reality, under high nutrient stress conditions, plants can exude nutrient carrier enzymes or facilitate mycorrhizal fungi associations to enhance competitiveness for nutrient acquisition [Drake *et al.*, 2011; Hobbie and Hobbie, 2006; Treseder and Vitousek, 2001]. In addition, plants can adjust C allocation to construct more fine roots, which scavenge nutrients over larger soil volumes [Iversen *et al.*, 2011; Jackson *et al.*, 2009; Norby *et al.*, 2004]. Soil spatial heterogeneity might also contribute to the success of plant nutrient competition [Korsaeth *et al.*, 2001]. Therefore, most ecosystem biogeochemistry models with traditional treatments of nutrient competition likely underestimate plant nutrient uptake.

Nutrient competition should be treated as a complex consumer-substrate reaction network: multiple ‘consumers’, including plant roots, soil heterotrophic microbes, nitrifiers, denitrifiers, and mineral surfaces, each competing for substrates of organic and inorganic nitrogen and phosphorus as nutrient supply. In such a model structure, the

success of any consumer in substrate acquisition is affected by its consumer-substrate affinity [Nedwell, 1999]. Such competitive interactions have been successfully applied to microbe-microbe and plant-microbe substrate competition modeling [Bonachela *et al.*, 2011; Lambers *et al.*, 2009; Maggi *et al.*, 2008; Maggi and Riley, 2009; Moorhead and Sinsabaugh, 2006; Reynolds and Pacala, 1993] for many years.

Here, we applied the consumer-substrate network in a broader context of plant, microorganism, and abiotic mineral interactions. We analyzed the consumer-substrate network using a first-order accurate equilibrium chemistry approximation (ECA) [Tang and Riley, 2013; Zhu and Riley, 2015]. Our sensitivity analysis confirmed that the consumer-substrate affinity and nutrient carrier enzyme abundance were the most important factors regulating relatively short-term competitive interactions. The ECA competition treatment represents ecosystem responses to environmental changes and has the potential to be linked to a microbe-explicit land biogeochemistry model. The approach allows competition between plants, microbes, and mineral surfaces to be prognostically determined based on nutrient status and capabilities of each consumer.

4. Conclusions

In this study, we developed a soil biogeochemistry model (N-COM) that resolves the dynamics of soil nitrogen and phosphorus, plant uptake of nutrients, microbial uptake, and abiotic interactions. We focused on the implementation, parameterization, and testing of the nutrient competition scheme that we plan to incorporate into the ESM land models CLM and ALM. We described the multiple-consumer and multiple-nutrient competition network with the Equilibrium Chemical Approximation (ECA) [Tang and Riley, 2013]

considering two inhibitive effects: (1) multiple substrates (*e.g.*, NH_4^+ and NO_3^-) sharing one consumer inhibits the effective binding between any specific substrate and the consumer and (2) multiple consumers (*e.g.*, plants, decomposing microbes, nitrifiers) sharing one substrate (*e.g.*, NH_4^+) lowers the probability of effective binding between any consumer and that substrate. We calibrated the model at a tropical forest site with highly weathered soil (Tapajos National Forest, Para, Brazil), using multiple observational datasets with the Markov Chain Monte Carlo (MCMC) approach. The model parameters were well constrained compared with their prior distributions (Table 4). The posterior parameter uncertainties were greatly reduced (on average by 75%). The posterior model compared to multiple categories of observational data was substantially improved over the prior model (Figure 4). The seasonal dynamics of soil carbon, nitrogen, and phosphorus were moderately well captured. However, our results would likely be more robust if more temporally resolved observations of carbon, nitrogen, and phosphorous were available in the individual consumer pools.

To test the resulting model using the posterior parameters, we applied N-COM to two other tropical forests (Hawaii tropical forest and Luquillo tropical forest) not used in the calibration process and conducted nutrient perturbation studies consistent with fertilization experiments at these sites. The results showed that N-COM simulated the nitrogen and phosphorus competition well for the majority of the observational metrics. However, the model underestimated NH_4^+ uptake by nitrifiers, probably due to the loosely constrained nitrification parameters that were the result of NO_3^- pool size data paucity during calibration at the Brazil site (Table 4). Datasets of soil nutrient pool sizes

and CO₂ and N₂O effluxes with high frequency sampling would significantly benefit the model uncertainty reduction.

To date, many terrestrial ecosystem biogeochemistry models assume microbes outcompete plants and immobilize nutrients first [Y P Wang *et al.*, 2007; Zaehle and Friend, 2010; Zhu and Zhuang, 2013], although CLM currently assumes constant and relative demand competitiveness of plants and microbes. Few models, to our knowledge, consider the role of abiotic interactions in the competitive interactions. In the case of microbes outcompeting plants, the plant is only able to utilize the nutrients that exceed microbial demands during that time step. The leftover nutrients are defined as net mineralization, which is a widely adopted concept in soil biogeochemistry modeling [Schimel and Bennett, 2004]. These models oversimplify plant-microbe interactions by imposing dubious assumptions (*e.g.*, microbes always win against plants). We showed that (in section 3.1) “competitiveness” is a dynamic rather than fixed property of the competition network, and more importantly, it should be linked to competitor functional traits (affinity and nutrient carrier enzyme abundance).

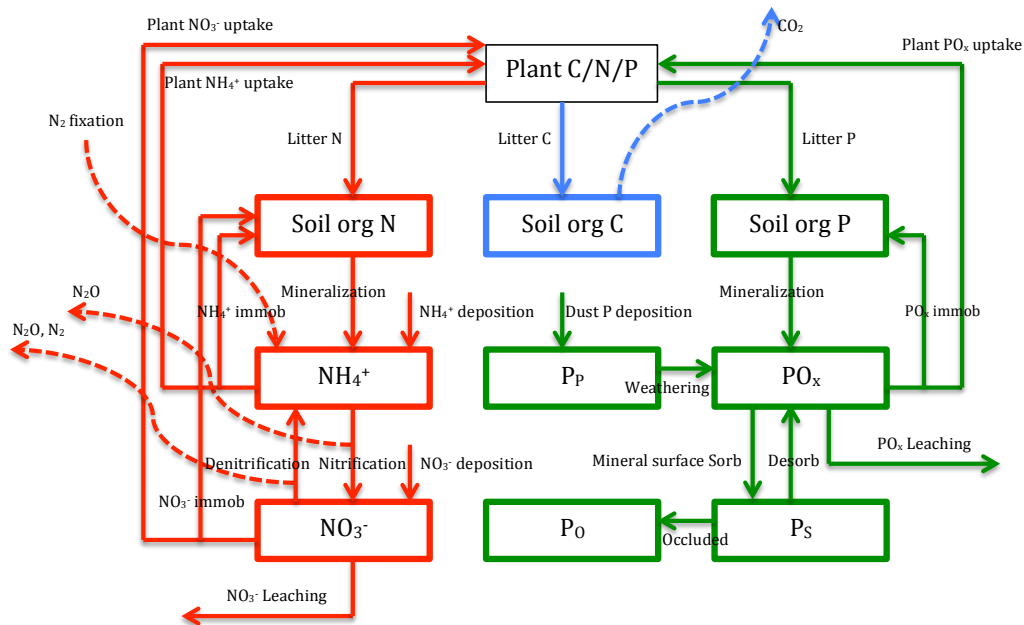
This study is a crucial step towards implementing more realistic nutrient competition schemes in complex climate-scale land models. Traditional ESMs generally lack realistic soil nutrient competition, which likely biases the estimates of terrestrial ecosystem carbon productivity and biosphere-climate feedbacks. This study showed the effectiveness of ECA kinetics in representing soil multiple-consumer and multiple-nutrient competition networks. Offline calibration and independent site-level testing is critically important to ensuring the newly incorporated model will perform reasonably when integrated in a complex ESM. To this end, we provide a universal calibration

676 approach using MCMC, which could in the future be used to further constrain N-COM
677 across plant functional types, climate, and soil types.

678

679 *Acknowledgements:* This research was supported by the Director, Office of Science,
680 Office of Biological and Environmental Research of the US Department of Energy under
681 Contract No. DE-AC02-05CH11231 as part of the Regional and Global Climate
682 Modeling (RGCM) and ACME programs.

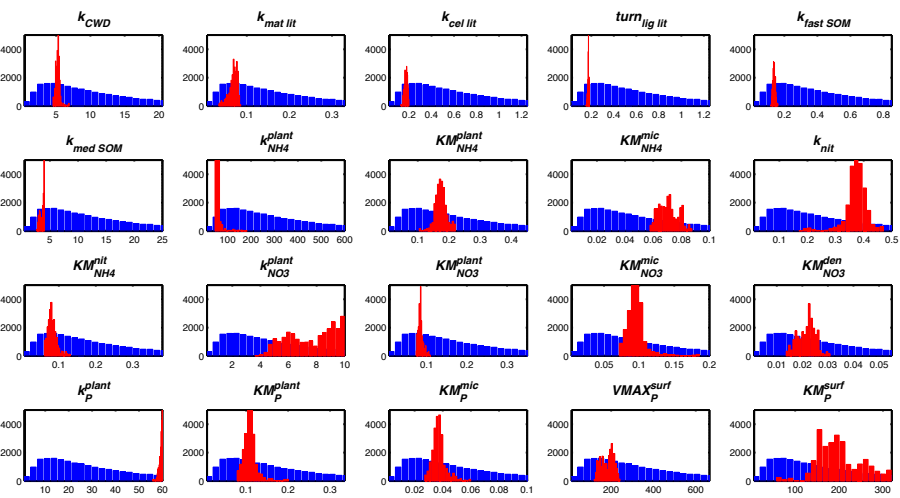
Figure 1. Model structure. Boxes represent pools, solid arrows represent aqueous fluxes, and dashed arrows represent gaseous pathways out or into the system. Three essential chemical elements (Carbon (C), Nitrogen (N) and Phosphorus (P)) are simulated in N-COM (blue, red, and green represent C, N, and P pools and processes, respectively).



Berkeley Lab 8/1/15 10:16 PM

Comment [1]: Figure is updated. "MIC NH₄ uptake", "MIC NO₃ uptake", "MIC PO_x" uptake are changed to "NH₄ immob", "NO₃ immob", and "PO_x immob"

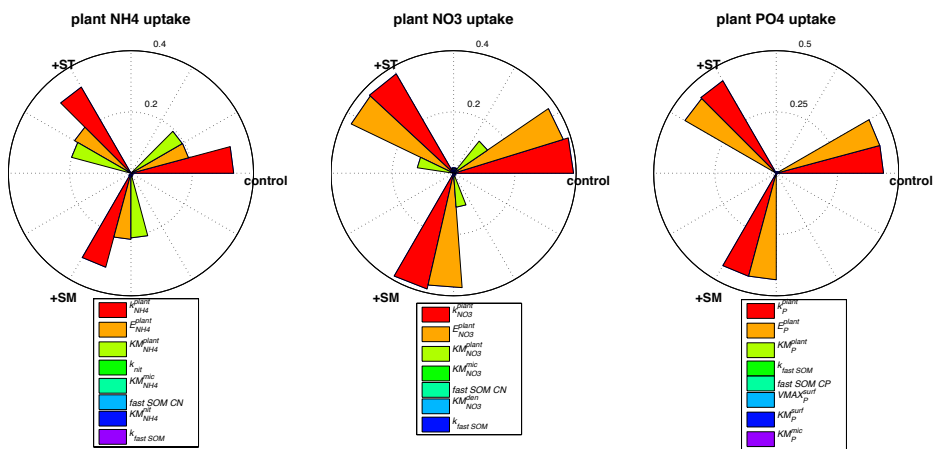
Figure 2. Distribution of prior and posterior model parameters.



Berkeley Lab 8/1/15 10:16 PM

Comment [2]: Figure is updated. Please note that prior and posterior distribution of parameters are plotted together for comparison.

690 **Figure 3.** Model sensitivity analysis with SOBOL sampling. For each metric, three
691 scenarios are shown: baseline (Control), elevated soil temperature by 5 °C (+ T_s), and
692 elevated soil moisture by 50% (+ θ), respectively. The length of bar (plot in polar
693 coordinate) is the sensitivity (unit-less) of model output with respect to model input
694 variables. Our results showed that the plant nutrient uptake was mostly regulated by
695 internal consumer-substrate uptake kinetics rather than the external environmental
696 conditions (*e.g.*, T_s , θ).



698 **Figure 4.** Model performance at Tapajos National Forest, Para, Brazil. Overall, the
699 posterior model (blue line) improved predictions over the prior model (grey line) when
700 compared to observations. Green areas indicate the posterior model uncertainties.

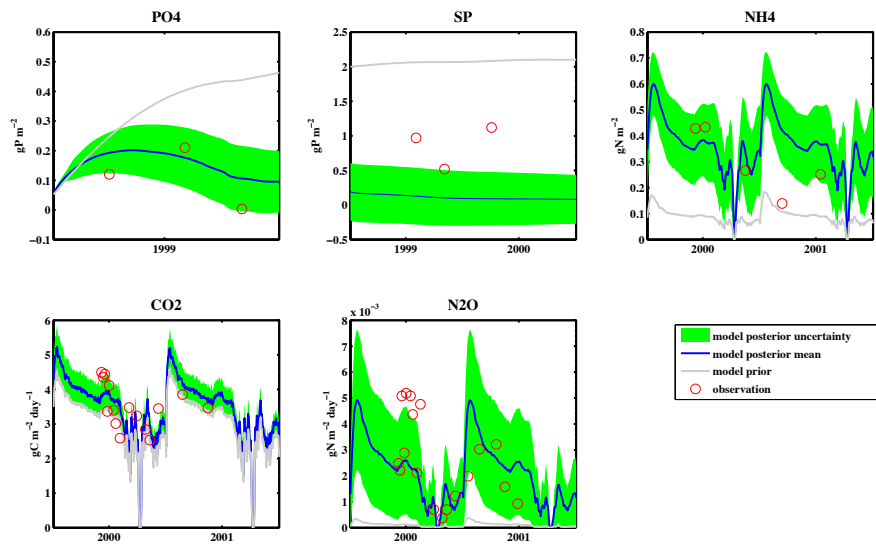
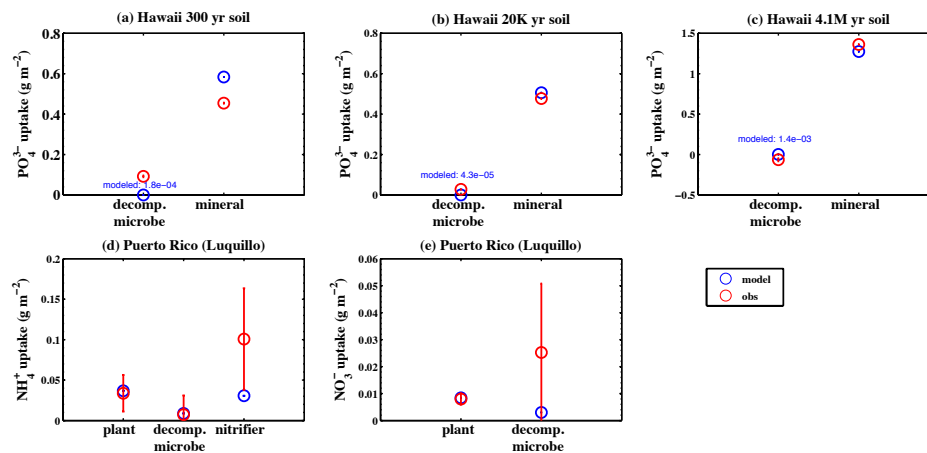


Figure 5. Model perturbation experiments compared with nitrogen and phosphorus

fertilization field experimental data. The blue dots show the difference between control and perturbed simulations, which mean how much newly added nutrient each consumer takes up. The red circles are recovered isotopically labeled nutrient within each consumer. Since plants phosphorus uptake was not measured at Hawaii sites, we didn't include the plants in the perturbation study.



Berkeley Lab 7/31/15 2:07 PM

Comment [5]: Figure is updated

709 **Table 1.** A summary of the modeled consumer-resource competition network.

Resources		Consumers	
NH ₄ ⁺	Plant	Decomposing Microbe	Nitrifier
NO ₃ ⁻	Plant	Decomposing Microbe	Denitrifier
PO _x	Plant	Decomposing Microbe	Mineral surface

710

Table 2. Model parameters and baseline values.

<i>C associated</i>				
g_i	Percentage of carbon remains in the soil after decomposition of i^{th} SOM	-	[1.0; 0.45; 0.5; 0.5; 0.83; 0.45; 0.45]	[Koven <i>et al.</i> , 2013]
f_{ij}	fraction of SOM leave from i^{th} pool and enter into j^{th} pool	-	[0, 0, 0.76, 0.24, 0, 0, 0; 0, 0, 0, 0, 1, 0, 0; 0, 0, 0, 0, 1, 0, 0; 0, 0, 0, 0, 0, 1, 0; 0, 0, 0, 0, 0, 0.995, 0.005; 0, 0, 0, 0, 0.93, 0, 0.07; 0, 0, 0, 0, 1, 0, 0]	[Koven <i>et al.</i> , 2013]
CN	Soil organic matter CN ratio	-	[13,16,7.9]	[Parton <i>et al.</i> , 1988]
CP	Soil organic matter CP ratio	-	[110,320,114]	[Parton <i>et al.</i> , 1988]
$TURN_{SOM}$	Soil organic matter turn over [CWD, metabolic lit, cellulose lit, lignin lit, fast SOM, medium SOM, slow SOM]	year	[4.1, 0.066, 0.25, 0.25, 0.17, 5, 270]	[Koven <i>et al.</i> , 2013]
<i>N associated</i>				
$k_{NH_4}^{plant}$	Reaction rate of plant NH_4^+ carrier enzyme	day ⁻¹	120 ^(a)	[Jackson <i>et al.</i> , 1997; Min <i>et al.</i> , 2000]
$KM_{NH_4}^{plant}$	Half-saturation constant for plant NH_4^+ uptake	g m ⁻²	0.09	[Kuzuyakov and Xu, 2013]
$KM_{NH_4}^{mic}$	Half-saturation constant for decomposing microbe NH_4^+ immobilization	g m ⁻²	0.02	[Kuzuyakov and Xu, 2013]
k_{nit}	Maximum fraction of NH_4^+ pool that could be utilized by nitrifiers	day ⁻¹	10%	[Parton <i>et al.</i> , 2001]
$KM_{NH_4}^{nit}$	Half-saturation constant for nitrifier NH_4^+ consumption	g m ⁻²	0.076	[Drtil <i>et al.</i> , 1993]
$k_{NO_3}^{plant}$	Reaction rate of plant NO_3^- carrier enzyme	day ⁻¹	2 ^(a)	[Jackson <i>et al.</i> , 1997; Min <i>et al.</i> , 2000]
$KM_{NO_3}^{plant}$	Half-saturation constant for plant NO_3^- uptake	g m ⁻²	0.07	[Kuzuyakov and Xu, 2013]
$KM_{NO_3}^{mic}$	Half-saturation constant for decomposing microbe NO_3^- immobilization	g m ⁻²	0.04	[Kuzuyakov and Xu, 2013]
$KM_{NO_3}^{den}$	Half-saturation constant for denitrifier NO_3^- consumption	g m ⁻²	0.011	[Murray <i>et al.</i> , 1989]
$[E_N^{plant}]$	Plant nitrogen carrier enzyme abundance for nitrogen uptake	g m ⁻²	$C_{\text{root}} \cdot 0.0000125^{(a)}$	[Tang and Riley, 2013; Trumbore <i>et al.</i> , 2006]
$[E_N^{mic}]$	Decomposing microbes nitrogen carrier enzyme abundance for nitrogen immobilization	g m ⁻²	$\frac{F_{N, \text{immob}, \text{pot}}}{1000}^{(b)}$	[Tang and Riley, 2013]
$[E_N^{nit}]$	Nitrifier nitrogen carrier enzyme abundance for NH_4^+ assimilation	g m ⁻²	$1.2E^{-3}$	[Raynaud <i>et al.</i> , 2006]

Berkeley Lab 7/31/15 2:07 PM

Comment [6]: Table is updated

$[E_N^{den}]$	Denitrifier nitrogen carrier enzyme abundance for NO_3^- assimilation	g m^{-2}	1.2E^{-3}	[Raynaud et al., 2006]
$f_{\text{N}_2\text{O}}$	Fraction of nitrification flux lost as N_2O	-	6E^{-4}	[Li et al., 2000]
P associated				
k_{weather}	Parent material P weathering rate	$\text{g P m}^{-2} \text{year}^{-1}$	0.004	[Y P Wang et al., 2010]
k_{occl}	P occlude rate	month^{-1}	1.0E^{-6}	[Yang et al., 2014]
k_p^{plant}	Reaction rate of plant PO_x carrier enzyme	day^{-1}	12 ^(a)	[Colpaert et al., 1999]
KM_p^{plant}	Half-saturation constant for plant PO_x uptake	g m^{-2}	0.067	[Cogliatti and Clarkson, 1983]
KM_p^{mic}	Half-saturation constant for decomposing microbe PO_x immobilization	g m^{-2}	0.02	[Chen, 1974]
$VMAX_p^{\text{surf}}$	Maximum mineral surface PO_x adsorption	g m^{-2}	133	[Y P Wang et al., 2010]
KM_p^{surf}	Half-saturation constant for mineral surface PO_x adsorption	g m^{-2}	64	[Y P Wang et al., 2010]
$[E_p^{\text{plant}}]$	Plant phosphorus carrier enzyme abundance for PO_x uptake	g m^{-2}	$C_{\text{froot}} \cdot 0.0000125$ ^(a)	[Tang and Riley, 2013; Trumbore et al., 2006]
$[E_p^{\text{mic}}]$	Decomposing microbes phosphorus carrier enzyme abundance for PO_x immobilization	g m^{-2}	$\frac{F_p^{\text{immob.pot}}}{800}$ ^(b)	[Tang and Riley, 2013]
$[E_p^{\text{surf}}]$	Mineral surface “effective enzyme” abundance for PO_x adsorption	g m^{-2}	$VMAX_p^{\text{surf}} - [SP]$	[Tang and Riley, 2013]

(a) The scaling factor for plant nutrient enzyme abundance is 0.0000125. This number is inferred by assuming that growing season plant nutrient carrier enzymes are roughly the same order of magnitude compared with decomposing microbes'. Typical values for soil decomposing microbe biomass and tropical forest fine root biomass are 0.1 [Tang and Riley, 2013] and 400 [Trumbore et al., 2006] gC m^{-2} . A typical value of scaling factor that scales microbial biomass to enzyme abundance is 0.05 [Tang and Riley, 2013]. Therefore, $C_{\text{froot}} \cdot x = C_{\text{mic}} \cdot 0.05$ or $400 \cdot x = 0.1 \cdot 0.05$. We have

$x = 0.0000125$. Further, we have $k_{\text{NH}_4}^{\text{plant}} \cdot [E_N^{\text{plant}}] = VMAX_{\text{NH}_4}^{\text{plant}}$. We know that typical values for $VMAX_{\text{NH}_4}^{\text{plant}}$ and $[E_N^{\text{plant}}]$ are $0.6 \text{ g m}^{-2} \text{day}^{-1}$ [Min et al., 2000] and 0.005 g m^{-2} . Then we have $k_{\text{NH}_4}^{\text{plant}} = 120 \text{ day}^{-1}$. Similarly, we have $k_{\text{NO}_3}^{\text{plant}} \cdot [E_N^{\text{plant}}] = VMAX_{\text{NO}_3}^{\text{plant}}$, $k_p^{\text{plant}} \cdot [E_p^{\text{plant}}] = VMAX_p^{\text{plant}}$. Knowing that typical values for $VMAX_{\text{NO}_3}^{\text{plant}}$ and $VMAX_p^{\text{plant}}$ are 0.01 [Min et al., 2000] and 0.06 [Colpaert et al., 1999] $\text{g m}^{-2} \text{day}^{-1}$, we have $k_{\text{NO}_3}^{\text{plant}} = 2$ and $k_p^{\text{plant}} = 12 \text{ day}^{-1}$.

(b) For decomposing microbes, we have $VMAX_N^{\text{mic}} = k_N^{\text{mic}} \cdot [E_N^{\text{mic}}]$. Typical values for $VMAX_N^{\text{mic}}$ and $[E_N^{\text{mic}}]$ are $5 \text{ g m}^{-2} \text{day}^{-1}$ [Kuzakov and Xu, 2013] and 0.005 g m^{-2} [Tang and Riley, 2013].

Therefore, we have $k_N^{\text{mic}} = 1000$. Since our model calculates potential N immobilization rates and approximates them as $VMAX_N^{\text{mic}}$. The changes of potential N immobilization rates at each time step

imply the changes of enzyme abundance through $[E_N^{\text{mic}}] = \frac{F_N^{\text{immob.pot}}}{k_N^{\text{mic}}} = \frac{F_N^{\text{immob.pot}}}{1000}$. Similarly, we have that $VMAX_p^{\text{mic}}$ and $[E_N^{\text{mic}}]$ are $2 \text{ g m}^{-2} \text{day}^{-1}$ [Chen, 1974] and 0.005 g m^{-2} . Therefore, $k_p^{\text{mic}} = 800$

and $E_p^{\text{mic}} = \frac{F_p^{\text{immob.pot}}}{800}$.

712 **Table 3.** Observational datasets used for calibration.

Processes	Datasets		Location	References
C associated	Soil heterotrophic respiration		Tapajos National Forest, Para, Brazil	[Silver <i>et al.</i> , 2012]
N associated	Soil NH ₄ ⁺	N ₂ O efflux	Tapajos National Forest, Para, Brazil	[Silver <i>et al.</i> , 2012]
P associated	Soil free phosphate	Sorb phosphate	Tapajos National Forest, Para, Brazil	[McGroddy <i>et al.</i> , 2008]

713

714 **Table 4.** Calibrated model parameters, prior mean, posterior means, and uncertainty

715 reduction after assimilating the observational datasets.

Berkeley Lab 7/31/15 2:07 PM

Comment [7]: Table is updated

Parameters	μ_{prior}	σ_{prior}	$\mu_{posterior}$	$\sigma_{posterior}$	Uncertainty Reduction %
$TURN_{SOM}$	[3.7, 0.06, 0.23,	[3.9, 0.06, 0.24,	[5.2, 0.07, 0.17,	[0.33, 0.01, 0.01,	[92, 83, 96, 98, 96,
[CWD, metabolic	0.23,0.16, 4.6]	0.24, 0.18, 4.8]	0.17, 0.14, 3.6]	0.005, 0.008, 0.37]	92]
lit, cellulose lit,					
lignin lit, fast					
SOM, medium					
SOM]					
$k_{NH_4}^{plant}$	109	114	58	14	88
$KM_{NH_4}^{plant}$	0.082	0.086	0.173	0.018	79
$KM_{NH_4}^{mic}$	0.018	0.019	0.071	0.0067	65
k_{nit}	0.091	0.095	0.37	0.038	60
$KM_{NH_4}^{nit}$	0.069	0.072	0.082	0.012	83
$k_{NO_3}^{plant}$	1.8	1.9	7.6	1.7	13
$KM_{NO_3}^{plant}$	0.064	0.067	0.085	0.0064	90
$KM_{NO_3}^{mic}$	0.036	0.038	0.096	0.014	63
$KM_{NO_3}^{den}$	0.0101	0.0105	0.022	0.0034	68
k_p^{plant}	11	11.5	59	0.75	93
KM_p^{plant}	0.061	0.064	0.11	0.015	77
KM_p^{mic}	0.018	0.019	0.037	0.0047	75
$VMAX_p^{surf}$	121	127	182	30	76
KM_p^{surf}	64	58	200	50	18

717 **Table 5.** Short-term (24 or 48 hours) fertilization experiments of NH_4^+ , NO_3^- , or PO_4^{3-}
 718 additions used to evaluate the performance of the N-COM competition scheme.

Datasets	Added nutrient	Competitors			Duration (hour)	References
PO_4^{3-} fertilization	$10\text{ }\mu\text{g g}^{-1}$	I. Mineral surface	II. Decomposing microbe		48	[Olander and Vitousek, 2005]
NH_4^+ fertilization	$4.6\text{ }\mu\text{g g}^{-1}$	I. Plant	II. Decomposing microbe	III. Nitrifier	24	[Templer et al., 2008]
NO_3^- fertilization	$0.92\text{ }\mu\text{g g}^{-1}$	I. Plant	II. Decomposing microbe		24	[Templer et al., 2008]

719

References:

- Anav, A., P. Friedlingstein, M. Kidston, L. Bopp, P. Ciais, P. Cox, C. Jones, M. Jung, R. Myneni, and Z. Zhu (2013), Evaluating the land and ocean components of the global carbon cycle in the CMIP5 Earth System Models, *Journal of Climate*, 26(18), 6801-6843.
- Bonachela, J. A., M. Raghieb, and S. A. Levin (2011), Dynamic model of flexible phytoplankton nutrient uptake, *Proceedings of the National Academy of Sciences*, 108(51), 20633-20638.
- Bonan, G. B., and K. V. Cleve (1992), Soil temperature, nitrogen mineralization, and carbon source-sink relationships in boreal forests, *Canadian Journal of Forest Research*, 22(5), 629-639.
- Chauhan, B. S., J. W. B. Stewart, and E. A. Paul (1981), Effect of labile inorganic phosphate status and organic carbon additions on the microbial uptake of phosphorus in soils, *Canadian Journal of Soil Science*, 61(2), 373-385.
- Chaves, M. M., J. P. Maroco, and J. S. Pereira (2003), Understanding plant responses to drought—from genes to the whole plant, *Functional plant biology*, 30(3), 239-264.
- Chen, M. (1974), Kinetics of phosphorus absorption by *Corynebacterium bovis*, *Microbial ecology*, 1(1), 164-175.
- Cogliatti, D. H., and D. T. Clarkson (1983), Physiological changes in, and phosphate uptake by potato plants during development of, and recovery from phosphate deficiency, *Physiologia plantarum*, 58(3), 287-294.
- Colpaert, J. V., K. K. Van Tichelen, J. A. Van Assche, and A. Van Laere (1999), Short-term phosphorus uptake rates in mycorrhizal and non-mycorrhizal roots of intact *Pinus sylvestris* seedlings, *New Phytologist*, 143(3), 589-597.
- DeLuca, T. H., O. Zackrisson, M. J. Gundale, and M.-C. Nilsson (2008), Ecosystem feedbacks and nitrogen fixation in boreal forests, *Science*, 320(5880), 1181-1181.
- DeLuca, T. H., O. Zackrisson, M.-C. Nilsson, and A. Sellstedt (2002), Quantifying nitrogen-fixation in feather moss carpets of boreal forests, *Nature*, 419(6910), 917-920.
- Dise, N. B., and R. F. Wright (1995), Nitrogen leaching from European forests in relation to nitrogen deposition, *Forest Ecology and Management*, 71(1), 153-161.
- Drake, J. E., A. Gallet - Budynek, K. S. Hofmockel, E. S. Bernhardt, S. A. Billings, R. B. Jackson, K. S. Johnsen, J. Lichter, H. R. McCarthy, and M. L. McCormack (2011), Increases in the flux of carbon belowground stimulate nitrogen uptake and sustain the long - term enhancement of forest productivity under elevated CO₂, *Ecology letters*, 14(4), 349-357.
- Drtil, M., P. Nemeth, and I. Bodik (1993), Kinetic constants of nitrification, *Water Research*, 27(1), 35-39.
- Elser, J. J., M. E. S. Bracken, E. E. Cleland, D. S. Gruner, W. S. Harpole, H. Hillebrand, J. T. Ngai, E. W. Seabloom, J. B. Shurin, and J. E. Smith (2007), Global analysis of nitrogen and phosphorus limitation of primary producers in freshwater, marine and terrestrial ecosystems, *Ecology letters*, 10(12), 1135-1142.

765 Friedlingstein, P., P. Cox, R. Betts, L. Bopp, W. Von Bloh, V. Brovkin, P. Cadule, S.
 766 Doney, M. Eby, and I. Fung (2006), Climate-carbon cycle feedback analysis:
 767 Results from the C4MIP model intercomparison, *Journal of Climate*, 19(14),
 768 3337-3353.
 769 Hobbie, J. E., and E. A. Hobbie (2006), 15N in symbiotic fungi and plants estimates
 770 nitrogen and carbon flux rates in arctic tundra, *Ecology*, 87(4), 816-822.
 771 Hodge, A., and A. H. Fitter (2010), Substantial nitrogen acquisition by arbuscular
 772 mycorrhizal fungi from organic material has implications for N cycling,
 773 *Proceedings of the National Academy of Sciences*, 107(31), 13754-13759.
 774 Hodge, A., D. Robinson, and A. Fitter (2000a), Are microorganisms more effective
 775 than plants at competing for nitrogen?, *Trends in plant science*, 5(7), 304-308.
 776 Hodge, A., J. Stewart, D. Robinson, B. S. Griffiths, and A. H. Fitter (2000b),
 777 Competition between roots and soil micro - organisms for nutrients from
 778 nitrogen - rich patches of varying complexity, *Journal of Ecology*, 88(1), 150-
 779 164.
 780 Houghton, R. A. (2003), Revised estimates of the annual net flux of carbon to the
 781 atmosphere from changes in land use and land management 1850-2000,
 782 *Tellus B*, 55(2), 378-390.
 783 Hu, S., F. S. Chapin, M. K. Firestone, C. B. Field, and N. R. Chiariello (2001), Nitrogen
 784 limitation of microbial decomposition in a grassland under elevated CO₂,
 785 *Nature*, 409(6817), 188-191.
 786 Iversen, C. M., T. D. Hooker, A. T. Classen, and R. J. Norby (2011), Net mineralization
 787 of N at deeper soil depths as a potential mechanism for sustained forest
 788 production under elevated [CO₂], *Global change biology*, 17(2), 1130-1139.
 789 Jackson, R. B., C. W. Cook, J. S. Pippen, and S. M. Palmer (2009), Increased
 790 belowground biomass and soil CO₂ fluxes after a decade of carbon dioxide
 791 enrichment in a warm-temperate forest, *Ecology*, 90(12), 3352-3366.
 792 Jackson, R. B., H. A. Mooney, and E. D. Schulze (1997), A global budget for fine root
 793 biomass, surface area, and nutrient contents, *Proceedings of the National*
 794 *Academy of Sciences*, 94(14), 7362-7366.
 795 Ji, D., et al. (2014), Description and basic evaluation of Beijing Normal University
 796 Earth System Model (BNU-ESM) version 1, *Geosci. Model Dev.*, 7(5), 2039-
 797 2064, doi:10.5194/gmd-7-2039-2014.
 798 Johnson, D. W. (1992), Nitrogen retention in forest soils, *Journal of Environmental*
 799 *Quality*, 21(1), 1-12.
 800 Kaspari, M., M. N. Garcia, K. E. Harms, M. Santana, S. J. Wright, and J. B. Yavitt (2008),
 801 Multiple nutrients limit litterfall and decomposition in a tropical forest,
 802 *Ecology Letters*, 11(1), 35-43.
 803 Kaye, J. P., and S. C. Hart (1997), Competition for nitrogen between plants and soil
 804 microorganisms, *Trends in Ecology & Evolution*, 12(4), 139-143.
 805 Korsaeath, A., L. Molstad, and L. R. Bakken (2001), Modelling the competition for
 806 nitrogen between plants and microflora as a function of soil heterogeneity,
 807 *Soil Biology and Biochemistry*, 33(2), 215-226.
 808 Koven, C. D., W. J. Riley, Z. M. Subin, J. Y. Tang, M. S. Torn, W. D. Collins, G. B. Bonan, D.
 809 M. Lawrence, and S. C. Swenson (2013), The effect of vertically resolved soil

810 biogeochemistry and alternate soil C and N models on C dynamics of CLM4,
811 *Biogeosciences*, 10, 7109-7131.

812 Kuzyakov, Y., and X. Xu (2013), Competition between roots and microorganisms for
813 nitrogen: mechanisms and ecological relevance, *New Phytologist*, 198(3),
814 656-669.

815 Lambers, H., C. Mougél, B. Jaillard, and P. Hinsinger (2009), Plant-microbe-soil
816 interactions in the rhizosphere: an evolutionary perspective, *Plant and Soil*,
817 321(1-2), 83-115.

818 Le Quéré, C., R. J. Andres, T. Boden, T. Conway, R. A. Houghton, J. I. House, G. Marland,
819 G. P. Peters, G. R. van der Werf, and A. Ahlström (2013), The global carbon
820 budget 1959–2011, *Earth System Science Data*, 5(1), 165-185.

821 Le Quéré, C., M. R. Raupach, J. G. Canadell, and G. Marland (2009), Trends in the
822 sources and sinks of carbon dioxide, *Nature Geoscience*, 2(12), 831-836.

823 LeBauer, D. S., and K. K. Treseder (2008), Nitrogen limitation of net primary
824 productivity in terrestrial ecosystems is globally distributed, *Ecology*, 89(2),
825 371-379.

826 Li, C., J. Aber, F. Stange, K. Butterbach - Bahl, and H. Papen (2000), A process -
827 oriented model of N₂O and NO emissions from forest soils: 1. Model
828 development, *Journal of Geophysical Research: Atmospheres* (1984-2012),
829 105(D4), 4369-4384.

830 Maggi, F., C. Gu, W. J. Riley, G. M. Hornberger, R. T. Venterea, T. Xu, N. Spycher, C.
831 Steefel, N. L. Miller, and C. M. Oldenburg (2008), A mechanistic treatment of
832 the dominant soil nitrogen cycling processes: Model development, testing,
833 and application, *Journal of Geophysical Research: Biogeosciences* (2005–2012),
834 113(G2).

835 Maggi, F., and W. J. Riley (2009), Transient competitive complexation in biological
836 kinetic isotope fractionation explains nonsteady isotopic effects: Theory and
837 application to denitrification in soils, *Journal of Geophysical Research:*
838 *Biogeosciences* (2005–2012), 114(G4).

839 Marion, G. M., P. C. Miller, J. Kummerow, and W. C. Oechel (1982), Competition for
840 nitrogen in a tussock tundra ecosystem, *Plant and soil*, 66(3), 317-327.

841 Marland, G., T. A. Boden, R. J. Andres, A. L. Brenkert, and C. A. Johnston (2003),
842 Global, regional, and national fossil fuel CO₂ emissions, *Trends: A*
843 *compendium of data on global change*, 34-43.

844 Matson, P., K. A. Lohse, and S. J. Hall (2002), The globalization of nitrogen
845 deposition: consequences for terrestrial ecosystems, *AMBIO: A Journal of the*
846 *Human Environment*, 31(2), 113-119.

847 Matson, P., W. H. McDowell, A. R. Townsend, and P. M. Vitousek (1999), The
848 globalization of N deposition: ecosystem consequences in tropical
849 environments, *Biogeochemistry*, 46(1-3), 67-83.

850 McGroddy, M. E., W. L. Silver, R. C. De Oliveira, W. Z. De Mello, and M. Keller (2008),
851 Retention of phosphorus in highly weathered soils under a lowland
852 Amazonian forest ecosystem, *Journal of Geophysical Research: Biogeosciences*
853 (2005–2012), 113(G4).

854 McGuire, A. D., J. M. Melillo, L. A. Joyce, D. W. Kicklighter, A. L. Grace, B. Moore, and C.
855 J. Vorosmarty (1992), Interactions between carbon and nitrogen dynamics in
856 estimating net primary productivity for potential vegetation in North
857 America, *Global Biogeochemical Cycles*, 6(2), 101-124.

858 Medvigy, D., S. C. Wofsy, J. W. Munger, D. Y. Hollinger, and P. R. Moorcroft (2009),
859 Mechanistic scaling of ecosystem function and dynamics in space and time:
860 Ecosystem Demography model version 2, *Journal of Geophysical Research:*
861 *Biogeosciences* (2005–2012), 114(G1).

862 Min, X., M. Y. Siddiqi, R. D. Guy, A. D. M. Glass, and H. J. Kronzucker (2000), A
863 comparative kinetic analysis of nitrate and ammonium influx in two early -
864 successional tree species of temperate and boreal forest ecosystems, *Plant,*
865 *Cell & Environment*, 23(3), 321-328.

866 Moorcroft, P. R., G. C. Hurtt, and S. W. Pacala (2001), A method for scaling vegetation
867 dynamics: the ecosystem demography model (ED), *Ecological monographs*,
868 71(4), 557-586.

869 Moorhead, D. L., and R. L. Sinsabaugh (2006), A theoretical model of litter decay and
870 microbial interaction, *Ecological Monographs*, 76(2), 151-174.

871 Mooshammer, M., W. Wanek, S. Zechmeister-Boltenstern, and A. Richter (2014),
872 Stoichiometric imbalances between terrestrial decomposer communities and
873 their resources: mechanisms and implications of microbial adaptations to
874 their resources, *Frontiers in microbiology*, 5.

875 Murray, R. E., L. L. Parsons, and M. S. Smith (1989), Kinetics of nitrate utilization by
876 mixed populations of denitrifying bacteria, *Applied and Environmental*
877 *Microbiology*, 55(3), 717-721.

878 Nedwell, D. B. (1999), Effect of low temperature on microbial growth: lowered
879 affinity for substrates limits growth at low temperature, *FEMS Microbiology*
880 *Ecology*, 30(2), 101-111.

881 Norby, R. J., J. Ledford, C. D. Reilly, N. E. Miller, and E. G. O'Neill (2004), Fine-root
882 production dominates response of a deciduous forest to atmospheric CO₂
883 enrichment, *Proceedings of the National Academy of Sciences of the United*
884 *States of America*, 101(26), 9689-9693.

885 Norby, R. J., J. M. Warren, C. M. Iversen, B. E. Medlyn, and R. E. McMurtrie (2010),
886 CO₂ enhancement of forest productivity constrained by limited nitrogen
887 availability, *Proceedings of the National Academy of Sciences*, 107(45), 19368-
888 19373.

889 Nordin, A., P. Högberg, and T. Näsholm (2001), Soil nitrogen form and plant nitrogen
890 uptake along a boreal forest productivity gradient, *Oecologia*, 129(1), 125-
891 132.

892 Olander, L. P., and P. M. Vitousek (2004), Biological and geochemical sinks for
893 phosphorus in soil from a wet tropical forest, *Ecosystems*, 7(4), 404-419.

894 Olander, L. P., and P. M. Vitousek (2005), Short-term controls over inorganic
895 phosphorus during soil and ecosystem development, *Soil Biology and*
896 *Biochemistry*, 37(4), 651-659.

897 Oren, R., D. S. Ellsworth, K. H. Johnsen, N. Phillips, B. E. Ewers, C. Maier, K. V. R.
898 Schäfer, H. McCarthy, G. Hendrey, and S. G. McNulty (2001), Soil fertility

899 limits carbon sequestration by forest ecosystems in a CO₂-enriched
 900 atmosphere, *Nature*, 411(6836), 469-472.
 901 Pappas, C., S. Fatichi, S. Leuzinger, A. Wolf, and P. Burlando (2013), Sensitivity
 902 analysis of a process - based ecosystem model: Pinpointing parameterization
 903 and structural issues, *Journal of Geophysical Research: Biogeosciences*, 118(2),
 904 505-528.
 905 Parton, W. J., E. A. Holland, S. J. Del Grosso, M. D. Hartman, R. E. Martin, A. R. Mosier,
 906 D. S. Ojima, and D. S. Schimel (2001), Generalized model for NO_x and N₂O
 907 emissions from soils, *Journal of Geophysical Research: Atmospheres* (1984–
 908 2012), 106(D15), 17403-17419.
 909 Parton, W. J., J. W. B. Stewart, and C. V. Cole (1988), Dynamics of C, N, P and S in
 910 grassland soils: a model, *Biogeochemistry*, 5(1), 109-131.
 911 Perakis, S. S., and L. O. Hedin (2002), Nitrogen loss from unpolluted South American
 912 forests mainly via dissolved organic compounds, *Nature*, 415(6870), 416-
 913 419.
 914 Phillips, R. P., A. C. Finzi, and E. S. Bernhardt (2011), Enhanced root exudation
 915 induces microbial feedbacks to N cycling in a pine forest under long - term
 916 CO₂ fumigation, *Ecology Letters*, 14(2), 187-194.
 917 Potter, C. S., J. T. Randerson, C. B. Field, P. A. Matson, P. M. Vitousek, H. A. Mooney,
 918 and S. A. Klooster (1993), Terrestrial ecosystem production: a process model
 919 based on global satellite and surface data, *Global Biogeochemical Cycles*, 7(4),
 920 811-841.
 921 Provides, G. F. W. I. (2014), Climate Model Intercomparisons: Preparing for the Next
 922 Phase, *Eos*, 95(9).
 923 Raynaud, X., J.-C. Lata, and P. W. Leadley (2006), Soil microbial loop and nutrient
 924 uptake by plants: a test using a coupled C: N model of plant-microbial
 925 interactions, *Plant and Soil*, 287(1-2), 95-116.
 926 Raynaud, X., and P. W. Leadley (2004), Soil characteristics play a key role in
 927 modeling nutrient competition in plant communities, *Ecology*, 85(8), 2200-
 928 2214.
 929 Reich, P. B., and S. E. Hobbie (2013), Decade-long soil nitrogen constraint on the CO₂
 930 fertilization of plant biomass, *Nature Climate Change*, 3(3), 278-282.
 931 Reich, P. B., S. E. Hobbie, T. Lee, D. S. Ellsworth, J. B. West, D. Tilman, J. M. H. Knops, S.
 932 Naeem, and J. Trost (2006), Nitrogen limitation constrains sustainability of
 933 ecosystem response to CO₂, *Nature*, 440(7086), 922-925.
 934 Reynolds, H. L., and S. W. Pacala (1993), An analytical treatment of root-to-shoot
 935 ratio and plant competition for soil nutrient and light, *American Naturalist*,
 936 51-70.
 937 Ricciuto, D. M., K. J. Davis, and K. Keller (2008), A Bayesian calibration of a simple
 938 carbon cycle model: The role of observations in estimating and reducing
 939 uncertainty, *Global biogeochemical cycles*, 22(2).
 940 Rillig, M. C., M. F. Allen, J. N. Klironomos, N. R. Chiariello, and C. B. Field (1998), Plant
 941 species-specific changes in root-inhabiting fungi in a California annual
 942 grassland: responses to elevated CO₂ and nutrients, *Oecologia*, 113(2), 252-
 943 259.

- Running, S. W., and J. C. Coughlan (1988), A general model of forest ecosystem processes for regional applications I. Hydrologic balance, canopy gas exchange and primary production processes, *Ecological modelling*, 42(2), 125-154.
- Schimel, J. P., and J. Bennett (2004), Nitrogen mineralization: challenges of a changing paradigm, *Ecology*, 85(3), 591-602.
- Schimel, J. P., L. E. Jackson, and M. K. Firestone (1989), Spatial and temporal effects on plant-microbial competition for inorganic nitrogen in a California annual grassland, *Soil Biology and Biochemistry*, 21(8), 1059-1066.
- Scholze, M., T. Kaminski, P. Rayner, W. Knorr, and R. Giering (2007), Propagating uncertainty through prognostic carbon cycle data assimilation system simulations, *Journal of Geophysical Research: Atmospheres* (1984–2012), 112(D17).
- Shen, J., L. Yuan, J. Zhang, H. Li, Z. Bai, X. Chen, W. Zhang, and F. Zhang (2011), Phosphorus dynamics: from soil to plant, *Plant physiology*, 156(3), 997-1005.
- Silver, W. L., A. W. Thompson, M. E. McGroddy, R. K. Varner, J. R. Robertson, H. S. J.D. Dias, P. Crill, and M. Keller (2012), LBA-ECO TG-07 Long-Term Soil Gas Flux and Root Mortality, Tapajos National Forest. Data set. Available on-line [<http://daac.ornl.gov>] from Oak Ridge National Laboratory Distributed Active Archive Center, Oak Ridge, Tennessee, U.S.A., <http://dx.doi.org/10.3334/ORNLDAAAC/1116>.
- Sokolov, A. P., D. W. Kicklighter, J. M. Melillo, B. S. Felzer, C. A. Schlosser, and T. W. Cronin (2008), Consequences of considering carbon-nitrogen interactions on the feedbacks between climate and the terrestrial carbon cycle, *Journal of Climate*, 21(15), 3776-3796.
- Springate, D. A., and P. X. Kover (2014), Plant responses to elevated temperatures: a field study on phenological sensitivity and fitness responses to simulated climate warming, *Global change biology*, 20(2), 456-465.
- Stocker, T. F., D. Qin, G.-K. Plattner, M. Tignor, S. K. Allen, J. Boschung, A. Nauels, Y. Xia, V. Bex, and P. M. Midgley (2013), Climate Change 2013. The Physical Science Basis. Working Group I Contribution to the Fifth Assessment Report of the Intergovernmental Panel on Climate Change-Abstract for decision-makers Rep., Groupe d'experts intergouvernemental sur l'évolution du climat/Intergovernmental Panel on Climate Change-IPCC, C/O World Meteorological Organization, 7bis Avenue de la Paix, CP 2300 CH-1211 Geneva 2 (Switzerland).
- Tang, J. Y., and W. J. Riley (2013), A total quasi-steady-state formulation of substrate uptake kinetics in complex networks and an example application to microbial litter decomposition, *Biogeosciences*, 10(12), 8329-8351, doi:10.5194/bg-10-8329-2013.
- Tang, J. Y., and W. J. Riley (2014), Weaker soil carbon-climate feedbacks resulting from microbial and abiotic interactions, *Nature Clim. Change*, advance online publication, doi:10.1038/nclimate2438 <http://www.nature.com/nclimate/journal/vaop/ncurrent/abs/nclimate2438.html> - supplementary-information.

989 Templer, P. H., W. L. Silver, J. Pett-Ridge, K. M. DeAngelis, and M. K. Firestone (2008),
 990 Plant and microbial controls on nitrogen retention and loss in a humid
 991 tropical forest, *Ecology*, 89(11), 3030-3040.
 992 Thomas, R. Q., G. B. Bonan, and C. L. Goodale (2013a), Insights into mechanisms
 993 governing forest carbon response to nitrogen deposition: a model-data
 994 comparison using observed responses to nitrogen addition, *Biogeosciences*
 995 *Discussions*, 10(1), 1635-1683.
 996 Thomas, R. Q., S. Zaehle, P. H. Templer, and C. L. Goodale (2013b), Global patterns of
 997 nitrogen limitation: confronting two global biogeochemical models with
 998 observations, *Global change biology*, 19(10), 2986-2998.
 999 Thornton, P. E., J. F. Lamarque, N. A. Rosenbloom, and N. M. Mahowald (2007),
 1000 Influence of carbon - nitrogen cycle coupling on land model response to CO₂
 1001 fertilization and climate variability, *Global Biogeochemical Cycles*, 21(4).
 1002 Treseder, K. K., and P. M. Vitousek (2001), Effects of soil nutrient availability on
 1003 investment in acquisition of N and P in Hawaiian rain forests, *Ecology*, 82(4),
 1004 946-954.
 1005 Trumbore, S., E. S. Da Costa, D. C. Nepstad, P. Barbosa De Camargo, L. A. Martinelli, D.
 1006 Ray, T. Restom, and W. Silver (2006), Dynamics of fine root carbon in
 1007 Amazonian tropical ecosystems and the contribution of roots to soil
 1008 respiration, *Global Change Biology*, 12(2), 217-229.
 1009 Vitousek, P. M., and H. Farrington (1997), Nutrient limitation and soil development:
 1010 experimental test of a biogeochemical theory, *Biogeochemistry*, 37(1), 63-75.
 1011 Vitousek, P. M., and R. W. Howarth (1991), Nitrogen limitation on land and in the
 1012 sea: how can it occur?, *Biogeochemistry*, 13(2), 87-115.
 1013 Vitousek, P. M., S. Porder, B. Z. Houlton, and O. A. Chadwick (2010), Terrestrial
 1014 phosphorus limitation: mechanisms, implications, and nitrogen-phosphorus
 1015 interactions, *Ecological applications*, 20(1), 5-15.
 1016 Vitousek, P. M., and R. L. Sanford (1986), Nutrient cycling in moist tropical forest,
 1017 *Annual review of Ecology and Systematics*, 137-167.
 1018 Waksman, S. A. (1931), Principles of soil microbiology, *Principles of soil*
 1019 *microbiology*.
 1020 Walker, T. W., and J. K. Syers (1976), The fate of phosphorus during pedogenesis,
 1021 *Geoderma*, 15(1), 1-19.
 1022 Wang, J., and B. Lars, R (1997), Competition for nitrogen during mineralization of
 1023 plant residues in soil: microbial response to C and N availability, *Soil Biology*
 1024 *and Biochemistry*, 29(2), 163-170.
 1025 Wang, Y. P., B. Z. Houlton, and C. B. Field (2007), A model of biogeochemical cycles of
 1026 carbon, nitrogen, and phosphorus including symbiotic nitrogen fixation and
 1027 phosphatase production, *Global Biogeochemical Cycles*, 21(1).
 1028 Wang, Y. P., R. M. Law, and B. Pak (2010), A global model of carbon, nitrogen and
 1029 phosphorus cycles for the terrestrial biosphere, *Biogeosciences*, 7(7), 2261-
 1030 2282.
 1031 Wieder, W. R., C. C. Cleveland, and A. R. Townsend (2009), Controls over leaf litter
 1032 decomposition in wet tropical forests, *Ecology*, 90(12), 3333-3341.

1033 Woodmansee, R. G., I. Vallis, and J. J. Mott (1981), Grassland nitrogen, *Ecological*
1034 *Bulletins (Sweden)*.

1035 Xu, X., P. E. Thornton, and W. M. Post (2013), A global analysis of soil microbial
1036 biomass carbon, nitrogen and phosphorus in terrestrial ecosystems, *Global*
1037 *Ecology and Biogeography*, 22(6), 737-749.

1038 Yang, X., P. E. Thornton, D. M. Ricciuto, and W. M. Post (2014), The role of
1039 phosphorus dynamics in tropical forests—a modeling study using CLM-CNP,
1040 *Biogeosciences*, 11(6), 1667-1681.

1041 Zaehle, S., and D. Dalmonech (2011), Carbon–nitrogen interactions on land at global
1042 scales: current understanding in modelling climate biosphere feedbacks,
1043 *Current Opinion in Environmental Sustainability*, 3(5), 311-320.

1044 Zaehle, S., P. Friedlingstein, and A. D. Friend (2010), Terrestrial nitrogen feedbacks
1045 may accelerate future climate change, *Geophysical Research Letters*, 37(1).

1046 Zaehle, S., and A. D. Friend (2010), Carbon and nitrogen cycle dynamics in the O -
1047 CN land surface model: 1. Model description, site - scale evaluation, and
1048 sensitivity to parameter estimates, *Global Biogeochemical Cycles*, 24(1).

1049 Zaehle, S., B. E. Medlyn, M. G. De Kauwe, A. P. Walker, M. C. Dietze, T. Hickler, Y. Luo,
1050 Y. P. Wang, B. El - Masri, and P. Thornton (2014), Evaluation of 11 terrestrial
1051 carbon-nitrogen cycle models against observations from two temperate
1052 Free - Air CO₂ Enrichment studies, *New Phytologist*, 202(3), 803-822.

1053 Zhang, Q., Y. P. Wang, A. J. Pitman, and Y. J. Dai (2011), Limitations of nitrogen and
1054 phosphorous on the terrestrial carbon uptake in the 20th century,
1055 *Geophysical Research Letters*, 38(22).

1056 Zhu, Q., and W. J. Riley (2015), Improved modelling of soil nitrogen losses, *Nature*
1057 *Climate Change*, 5(8), 705-706.

1058 Zhu, Q., and Q. Zhuang (2013), Modeling the effects of organic nitrogen uptake by
1059 plants on the carbon cycling of boreal ecosystems, *Biogeosciences*, 10(8),
1060 13455-13490.

1061 Zhu, Q., and Q. Zhuang (2014), Parameterization and sensitivity analysis of a
1062 process - based terrestrial ecosystem model using adjoint method, *Journal of*
1063 *Advances in Modeling Earth Systems*.

1064